NOVA SCHOOL OF SCIENCE & TECHNOLOGY

Department Of
Mechanical And Industrial Engineering

JOÃO FRANCISCO CUNHA ANDRÉ

BSc in Science of Mechanical Engineering

MEASURING ABSOLUTE SALINITY THROUGH DENSITY, REFRACTIVE INDEX, AND SOUND SPEED TRACEABILITY

MECHANICAL ENGINEERING INTEGRATED MASTER'S
NOVA Universidade de Lisboa
September, 2023

DEPARTMENT OF
MECHANICAL AND INDUSTRIAL ENGINEERING

MEASURING ABSOLUTE SALINITY THROUGH DENSITY, REFRACTIVE INDEX, AND SOUND SPEED TRACEABILITY

JOÃO FRANCISCO CUNHA ANDRÉ

BSc in Science of Mechanical Engineering

Adviser: Doctor Helena Víctorovna Guitiss Navas,
Assistant Professor, *NOVA School of Science and Technology*

Co-advisers: Doctor Andreia Filipa Morgado Furtado,
Technical Manager of the Liquid Properties Laboratory, IPQ

Examination Committee:

Chair: Doctor Rui Fernando dos Santos Pereira Martins,
Associate Professor, *NOVA School of Science and Technology*

Rapporteurs: Doctor Olivier Alain Geràrd Penedo Pellegrino,
Responsible of the Photometry, Radiometry and Radiofrequency laboratories at IPQ

Adviser: Doctor Helena Víctorovna Guitiss Navas,
Assistant Professor, *NOVA School of Science and Technology*

MECHANICAL ENGINEERING INTEGRATED MASTER'S

NOVA Universidade de Lisboa
September, 2023

MEASURING ABSOLUTE SALINITY THROUGH DENSI-TY, REFRACTIVE INDEX, AND SOUND SPEED TRACEABILITY

This document was created with Microsoft Word text processor and the NOVAthesis Word template.

Dedicated to my family and the stars in the sky that watch over me.

ACKNOWLEDGMENTS

With the completion of this dissertation, I reach the end of what has been, up until now, one of my main objectives. Therefore, I want to express my gratitude to all those who have contributed, directly or indirectly, and supported me in achieving this milestone.

A very special thanks to Doctor Andreia Furtado and Master Sara Moura for all the knowledge they imparted to me throughout this process and for always doing so with a great mood.

To my advisor, Professor Doctor Helena Navas, for the availability and constant support demonstrated during the elaboration of my dissertation.

To IPQ, which provided me with this unique opportunity to better understand how metrology works in Portugal.

To all the teachers who accompanied me during my academic journey.

To my family, my parents, and my sister who have always supported me throughout my life and academic journey, and to my friends without whom the journey would not have been the same.

“If I have seen further than others, it is by standing upon the shoulders of giants."
(Isaac Newton)

ABSTRACT

Speed of sound measurements have previously been used to derive seawater salinity and density over limited ranges where conductivity measurements have not been reliable. It has been conventional for several decades to derive the salinity of the seawater from measurements of conductivity. These measurements are only affected by the dissolved ionic, electrolytic, solutes in seawater, being the definition of absolute salinity the total mass fraction of all dissolved matter in the solution.

Several studies show the metrological compatibility of salinity results obtained by refractometry and densimetry. This study focuses on the validation of a new density and speed of sound measurement system (Anton Paar, DSA 5000M) and extends the applicable salinity range for determining salinity using refractometry and densimetry. Temperature calibration results established a tolerance of 0.038 °C within the range of [10, 40] °C.

Viscosity calibration showed negligible density errors for viscosity values in the range [0.66, 70.32] mPa s, but deviations up to 0.106 kg m^{-3} for higher viscosity values, suggesting the need for lower uncertainty calibration standards. Polynomial regressions facilitated the estimation of dynamic viscosity from density indications within the viscosity interval of [7, 220] mPa s with a relative standard uncertainty of 3 %.

The speed of sound measurements, calibrated with various substances, exhibited negligible errors in the Intervals [1255, 1484] m s^{-1} (maximum deviation of 0.2 %) and [1490, 1530] m s^{-1}, errors within 0.02 % to 0.42 % at 20 °C. The study also confirmed the metrological compatibility of absolute salinity values obtained by refractometry and densimetry measurements in the [5, 40] g kg^{-1} S_A interval, including seawater samples. Overall, this research contributes to enhancing the accuracy and applicability of density and speed of sound measurements in diverse scientific and industrial contexts.

Keywords Density, Metrology, Refractive index, Salinity, Seawater, Speed of sound.

RESUMO

As medições da velocidade do som foram usadas anteriormente para alcançar a salinidade e a massa volúmica da água do mar em intervalos limitados, onde as medições de condutividade não eram de confiança. É convencional há várias décadas alcançar a salinidade da água do mar a partir de medições de condutividade. Estas medições são afetadas apenas pelos solutos iônicos, eletrolíticos dissolvidos na água do mar, sendo a definição de salinidade absoluta a fração de massa total de toda a matéria dissolvida na água.

Vários estudos demostram a compatibilidade metrológica dos resultados de salinidade obtidos por refratometria e densimetria. O foco deste estudo é a validação de um novo densímetro e sistema de medição da velocidade do som (Anton Paar, DSA 5000M) e aumentar a faixa de salinidade aplicável para a determinação de salinidade usando refratometria e densimetria. Resultados de calibração de temperatura estabeleceram uma tolerância de 0.038 ^{o}C dentro do intervalo de [10, 40] ^{o}C.

A calibração de viscosidade mostrou erros de densidade negligenciáveis para valores de viscosidade no intervalo [0.66, 70,32] mPa s, mas desvios de até 0,106 kg m-3 para valores de viscosidade mais altos, sugerindo a necessidade de padrões de calibração com menor incerteza. Regressões polinomiais facilitaram a estimativa da viscosidade dinâmica a partir das indicações de densidade dentro do intervalo de viscosidade de [7 mPa s a 220 mPa s] com uma incerteza relativa padrão de 3 %.

As medições da velocidade do som, calibradas com várias substâncias, apresentaram erros insignificantes nos intervalos [1255, 1484] m s^{-1} (desvio máximo de 0.2 %) e [1490, 1530] m s^{-1}, erros entre 0.02 % e 0.42 % a 20 ^{o}C. O estudo também confirmou a compatibilidade metrológica dos valores de salinidade absoluta obtidos por refratometria e densimetria no intervalo [5; 40] g kg^{-1} de S_A, incluindo amostras de água do mar. No geral, esta pesquisa contribui para melhorar a precisão e a aplicabilidade de medidas de densidade e velocidade do som em diversos contextos científicos e industriais.

Palavras chave: Água do Mar, Índice de Refração, Massa Volúmica, Metrologia, Salinidade, Velocidade do Som

CONTENTS

LIST OF FIGURES

LIST OF TABLES

ACRONYMS

ADCP	Acoustic Doppler Current Profiler
BIPM	*Bureau international des poids et mesures*
CCD	Charge-Coupled Device
CGPM	General Conference on Weights and Measures
CIPM	International Committee for Weights and Measures
CRM	Certified Reference Material
DMET	*Departamento de Metrologia*
EURAMET	European Association of National Metrology Institutes
IPQ	*Instituto Português da Qualidade*
ISO	Internal Organization for Standardization
LED	Light-Emitting Diode
LFR	*Laboratório de Fotometria, Radiometria e Radiofrequências*
LNM	*Laboratório Nacional de Metrologia*
LPL	*Laboratório de Propriedades de Líquidos*
NIST	National Institute of Standards and Technology (USA)
OIML	International Organization of Legal Metrology
PRT	Platinum Resistance Thermometer
SC	Subcommittee
SI	*Système international d'unités*
SPQ	*Sistema Português da Qualidade*
SSW	Standard seawater
TC	Technical Committee
UNESCO	United Nations Educational, Scientific and Cultural Organization
VIM	*Vocabulaire International de Métrologie*

SYMBOLS

c	speed of sound (m s^{-1})
d	viscosity-corrected density indication (kg m^{-3})
d_{nc}	not viscosity-corrected density indication (kg m^{-3})
f	frequency (Hz)
k	coverage factor
m	mass (kg)
n	refractive index
P	pressure (kPa)
S	salinity (g kg^{-1})
t	temperature (^{o}C)
u	standard uncertainty
U	expanded uncertainty
V	volume (L)
ρ	density (kg m^{-3})
η	dynamic viscosity (mPa s)
$\bar{x}$	arithmetic mean

1

INTRODUCTION

In this chapter, a thorough introduction to the project will be presented. Here are specifically outlined the study's fundamental aspects, including the established framework, objectives, employed methodology, and the overall structural organization.

1.1 Motivation

The Earth's oceans are far more than just vast expanses of water; they are dynamic, living entities that have a profound impact on the very fabric of our planet. These immense bodies of water are not only awe-inspiring in their beauty but are also central to the intricate workings of Earth's ecosystems and climate systems. They are the driving force behind global weather patterns, a vital source of sustenance for countless species, and a regulator of the Earth's temperature. In essence, they are the beating heart of our planet.

To truly appreciate the significance of the oceans, we must journey into the realm of their physical properties. Salinity, density, refractive index, and speed of sound are not just scientific terms; they are the keys that unlock our understanding of the oceans and their influence on our world. These properties form the very foundation of various scientific disciplines, ranging from oceanography and marine biology to climate studies and resource exploration. They enable us to peer into the intricate mechanisms of ocean circulation, the transportation of heat across the globe, and the delicate balance that sustains marine life in the harshest of environments (National Geographic, 2023).

This study explores the theoretical underpinnings of density, refractive index, and speed of sound measurements. It reviews the existing literature on these topics and presents the employed methodologies. Additionally, the experimental setup, data analysis techniques, and the results obtained are discussed.

1.2 Study Objectives

The opportunity of this study appeared due to the ongoing collaboration between the *Instituto Português da Qualidade* (IPQ) and the NOVA School of Science and Technology. So the objectives of this study were multifaceted, encompassing a thorough investigation into the properties and capabilities of IPQ's new density meter and speed of sound measurement system, the Anton Paar DSA 5000M, more specifically they were:

- To validate the performance and reliability of IPQ new density and speed of sound measurement system, specifically assessing its accuracy in measuring the density of sodium chloride solutions at 20 ^{o}C within the [1001, 1027] kg m^{-3} density interval;
- To determine whether the density meter's readings required any correction, with a specific focus on viscosity correction. This objective aims to identify areas where improvements and further investigations might be necessary;
- To establish temperature calibration results, within the [10, 40] ^{o}C temperature interval;
- To investigate the calibration of viscosity and determine the range where density indications corrected for viscosity remain negligible and where deviations become significant ;
- To develop polynomial regression models to describe the relationship between density indication errors and dynamic viscosity, thereby enabling the estimation of viscosity for Newtonian liquids within the [7, 220] mPa s viscosity interval;
- To determine the speed of sound indication errors, focusing on the [255, 1484] m s^{-1} interval, when calibrated with specific substances, and comparing them to the associated uncertainty. Additionally, to analyse the errors within the [1490, 1530] m s^{-1} interval, when calibrated with aqueous solutions of NaCl and seawater dilutions, and assess the relative errors and uncertainties;
- To verify the metrological compatibility of absolute salinity, S_A, values obtained by refractometry and densimetry in the [5; 40] g kg^{-1} interval, including those derived from seawater samples.

These goals are the continuation of the *Laboratório de Propriedades dos Líquidos* (LPL)'s pursuit for better metrological traceable results.

1.3 Study Methodology

The study at hand unfolds in a comprehensive and structured manner, encompassing three distinct experimental segments, each contributing uniquely to our understanding of density and speed of sound measurements, and the intricate world of salinity assessment.

In the first segment the validation of density and speed of sound measurements are conducted, it is devoted to the validation of density and speed of sound measurement results, a task undertaken with the utilization of the DSA 5000 M instrument by Anton Paar. This phase sets the foundation for subsequent investigations, ensuring the accuracy and reliability of our data.

The second part consists of metrological compatibility of absolute salinity values. In this part, the focus shifts towards the realm of metrology, this segment is dedicated to the study of absolute salinity values, acquired through two distinct measurement techniques: refractometry and densimetry. The convergence of these methodologies is studied, gaining insights on their possible compatibility and providing new information into the world of salinity analysis.

The third and last experimental step consists of studying the matrix effect in absolute salinity determination. The investigation extends to a set of samples encompassing standard seawater (SSW), with crucial importance in oceanographic research. Comparing these samples to those in ultrapure water solutions, aimed to give new insights into the impact of matrix variations on absolute salinity determination were gained.

1.4 Dissertation Structure

This dissertation is organized into five different chapters.

This initial chapter serves as an introduction to the dissertation, where the framework of the study is established. It includes a concise description of the study's objectives, outlining its purpose. Furthermore, the chapter thoroughly explains the methods employed to achieve these objectives.

The second chapter, provides an introduction to Metrology, provides an overview of the field of metrology. By emphasis of the fundamentals of the International System of Units (SI). Additionally, it presents an overview of the organization of the metrology in Portugal, offering context to the subsequent analysis within the broader domain of regulatory frameworks.

The third chapter displays the Materials and Methods of the study, offering an understanding of the followed processes. It does so by providing a clear and organized explanation of the detailed steps taken during the research.

In the fourth chapter, named Results and Discussion, the investigation's findings are shown and elucidated.

In the final chapter, Conclusion, a summary and synthesis of the dissertation's key findings and insights are provided. It offers a concise culmination of the study, highlighting

its contributions and implications. This chapter also outlines potential avenues for future research within the field, offering a forward-looking perspective.

2

INTRODUCTION TO METROLOGY

In this chapter, an introduction to metrology is made along with an introduction to the International System of Units, the Organs of Quality in Portugal as well as the derived quantities that were measured.

2.1 Metrology

Metrology, defined by the International Vocabulary of Metrology (VIM) (JCGM 200:2012) as "the science of measurement and its application", encompasses both theoretical and practical aspects of measurement, spanning diverse fields and measurement uncertainties. In our daily lives, measurements and metrology play a fundamental role, underpinning a wide array of activities, including production control, environmental quality assessment, healthcare, safety evaluation, and ensuring the quality of materials, food, and consumer goods, to name but a few examples.

Indeed, metrology is the science that keeps airplanes flying safely, enabling high-speed technology and secure communications. It contributes to reducing the staggering number of annual deaths resulting from poorly calibrated medication dosing, amounting to thousands of lives lost. Furthermore, it protects consumers' wallets, ensuring fair pricing for consumed goods and services (IPQ, 2020).

The concepts inherent in these examples, along with their technical implications, represent merely a fraction of the situations encountered daily. Most of our actions and decisions, often taken unconsciously, rely heavily on the evaluation of surrounding quantities—a process fundamentally tied to measurement. The very essence of this evaluation lies in the art of measurement, where precise and accurate quantification is achieved through metrology.

2.2 The International System of Units

The International System of Units (SI) was formally defined and established by the 11th General Conference on Weights and Measures (CGPM) in 1960, with subsequent periodic revisions in response to user needs and scientific advancements. The most recent and significant revision of the SI was made by the 26th CGPM in 2018, documented in the 9th edition of the SI Brochure (BIPM,2022).

The SI is a consistent and universally recognized system of units applicable in various aspects of life, including international trade, manufacturing, security, health and safety, environmental protection, and fundamental scientific research. It is based on a set of seven defining constants, representing the most fundamental feature of the entire system of units.

These seven defining constants, chosen carefully to ensure accuracy and precision, form the basis for deriving the complete system of units are (BIPM, 2022):

- the unperturbed ground state hyperfine transition frequency of the caesium-133 atom, $\Delta \nu$ Cs =9 192 631 770 Hz
- the speed of light in vacuum, c= 299 792 458 m s^{-1}
- the Planck constant, h =6.626 070 15 · 10^{-34} J s
- the elementary charge, e= 1.602 176 634 ·10^{-19} C
- the Boltzmann constant, k = 1.380 649 ·10^{-23} J K^{-1}
- the Avogadro constant, N_A =6.022 140 76 ·1023 mol^{-1}
- the luminous efficacy of monochromatic radiation of frequency 540 ·10^{12} Hz, K_{cd} = 683 lm/W

Each base unit, can be defined in terms of these constants, demonstrating the coherency of the SI system as is shown in figure 2-1 below.

Figure 2-1 SI logo

(BIPM (a), 2022)

The realization of SI units is achieved through a variety of experimental methods described by the International Committee for Weights and Measures (CIPM) Consultative Committees, referred to as "mises en pratique." These realizations may be revised as new experiments are developed, ensuring continuous improvement and accuracy. The SI is an essential

tool in various fields, ensuring consistent and accurate measurements worldwide, and its periodic revisions demonstrate its adaptability to evolving scientific knowledge and technological advancements (BIPM (b), 2022).

2.3 Salinity

The Earth's oceans, play a critical role in shaping our planet's climate, supporting diverse ecosystems, and influencing global weather patterns. A fundamental property that governs seawater's behavior and composition is its salinity, which refers to the mass of dissolved salts in a saline solution divided by the mass of the solution. Salinity values vary widely, ranging from a few grams per kilogram in rivers and lakes to 35 g kg^{-1} in seawater, and even higher values for brine, such as around 260 g kg^{-1} (Furtado *et al.*, 2022).

Within the realm of salinity, two primary types can be defined: absolute salinity, S_A, and practical salinity, S. Absolute salinity represents the total amount of dissolved salts present in the solution, while practical salinity is calculated solely from conductive components. For oceanographic applications, absolute salinity, S_A holds distinct advantages over practical salinity S for oceanographic purposes. For instance, S_A has no limitations by scale, improves ocean models (as S_A is truly conservative), and enables reducing density errors in the Equation of State for seawater. Hence, new algorithms have been formulated for density, enthalpy, entropy, potential temperature, and sound speed in terms of absolute salinity, temperature and pressure (Feistel, 2008).

As seawater relative chemical composition is roughly uniform around the world (Nayar *et al.*, 2016), it is allowed to treat seawater as an aqueous solution of a single salt concentration by using the absolute salinity, S_A, (Millero *et al.*, 2008). However, mass fraction of dissolved salts in seawater or other natural water is not easy to measure directly due to the difficulty of drying the salts from these waters. Consequently, the salinity is usually calculated from other quantities, such as chlorinity or electrical conductivity (IUPAC, 2008). Nevertheless, the magnitudes of the uncertainty of these two quantities are still not fit for oceanographic purposes. On the other hand, among the experimental techniques that enable a quantitative analysis of aqueous solutions, densimetry and refractometry have shown to be reliable and easy to use for sodium chloride aqueous solutions (Furtado *et al.*, 2022).

2.4 Derived quantities measured

For this study, three different derived quantities were measured: density, refractive index, and speed of sound. These quantities were then used to determine salinity of the test samples. In the following sub-chapters, each one will be described concerning its definition, metrological traceability and measurement method used in this study.

2.4.1 Density

Density, ρ, is a fundamental property defined as the ratio of an object's mass, m, to its volume, V, denoted as $\rho = m/V$. The unit of density is kg m^{-3}. In various applications, especially in liquids, mass is often determined based on volume and density measurements. The required relative standard uncertainty of density measurements varies according to the field of study. For instance, in oceanography, relative uncertainties lower than $1 \cdot 10^{-5}$ are essential to study ocean currents caused by density variations. Reference tables and formulas for water density enable the use of ultra-pure water as a density standard with a low relative uncertainty of $1 \cdot 10^{-5}$ (Bettin, Borys & Nicolaus, 2008).

The hierarchy arrangement governing the propagation of the density unit, spanning the range of 0.5 kg m^{-3} to 24 000 kg m^{-3}, has been meticulously devised by the OIML Subcommittee SC4 ("Densities"), within the framework of the Technical Committee TC9 ("Instruments for measuring mass and density"). This international recommendation, illustrated in Figure 2-2, establishes a systematic approach for actualizing the density unit through the absolute method, utilizing the base units of mass and length. The primary standard for the density unit is connected to primary standards for length and mass units. Countries without primary standard equipment can utilize secondary density standards, and so forth. This framework ensures the consistent realization of the density unit across various levels of measurement standards and instruments (Ehlers *et al.*, 2019).

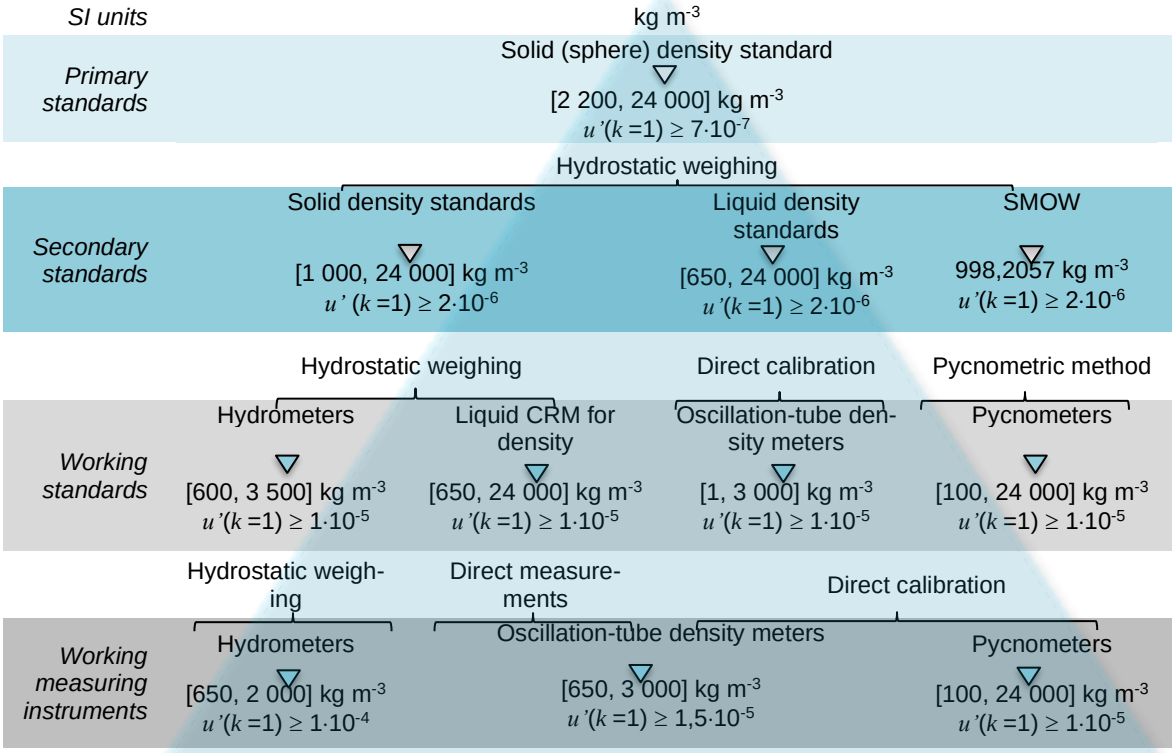

Figure 2-2 Hierarchy scheme of dissemination of the density unit for liquids (Furtado, 2019).

Between all these methods, in this study, only oscillation-type density meters were used to measure density. Oscillation-type density meters employ the fundamental law of harmonic oscillation (Stabinger, 1994) as their cornerstone measurement principle. These instruments utilize a measuring cell that acts as a flexural oscillator, filled with the sample fluid and subjected to oscillatory forces. The cell's oscillation frequency, determined by its own fundamental properties and influenced by the sample's characteristics, offers insights into density (Figure 2-3).

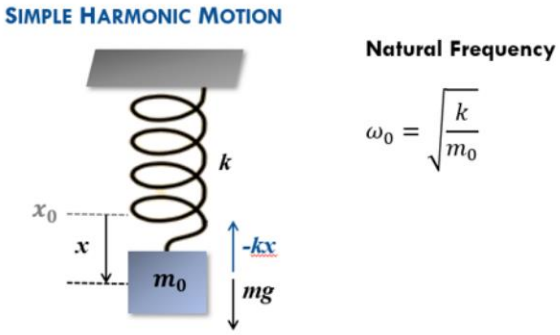

Figure 2-3 Measurement principle of the oscillation-type density meter (Furtado, 2019).

The measuring principle is reminiscent of simple harmonic motion described by the following equations (II.1 and II.2):

$$f = \frac{1}{2\pi}\sqrt{\frac{k}{M_0 + \rho V}} \qquad \text{II.1}$$

$$\tau = 2\pi\sqrt{\frac{M_0 + \rho V}{k}} \qquad \text{II.2}$$

Where:

f is the oscillation frequency;

M_0 is the mass of the oscillator;

ρ is the density of the test liquid;

τ is the oscillation period;

V is the volume of the oscillator;

k is the stiffness of the oscillator.

Where a mass ,M_0, attached to a spring with stiffness k oscillates around an equilibrium position x_0. The system's natural frequency ω_0 is dependent on the spring constant and mass. When filled with a test liquid of density ρ, the system's mass becomes $M = M_0 + \rho V$, leading

to changes in oscillation frequency. The oscillation period, τ obtained from the oscillation frequency, forms the basis for deriving the density of the measured liquid.

In these devices, the mass-spring model governs the relationship between oscillation period, τ, density, ρ, and the oscillation period, k. This relation is characterized by a second-order empirical equation, and the constants A and B are determined through calibration with reference fluids of known densities (Eq. 2.3-5).

$$\rho(t,p) = \mathrm{A}(t,p)\tau^2 - \mathrm{B}(t,p) \quad \text{(Eq.2.3)}$$

$$A = \frac{k(t,p)}{4\pi^2 V(t,p)} \quad \text{(Eq.2.4)}$$

$$B = \frac{M_0}{V(t,p)} \quad \text{(Eq.2.5)}$$

Where:

A and B are constants of the oscillator determined through calibration with reference fluids of known densities.

The viscous behavior of the fluid during oscillation introduces damping, altering the resonance frequency of the system. To mitigate this effect, certain density meters induce oscillation at higher harmonics, allowing for damping correction. From these data, density meters derive both viscosity-corrected, d and not viscosity-corrected, d_{nc} density values.

The empirical relation (Eq. 2.3) links density to the square of the oscillation period, with constants A and B defined through calibration against reference liquids of known densities. The principle's theoretical basis has implications for design challenges, accurate modeling, and accuracy enhancement. While complex, it underscores the importance of calibration and constant refinement in achieving precise density measurements, ensuring reliability in various scientific and industrial applications. However different types of mathematical models for both the calibration of the oscillators and the density calculations can be used, these can be found in (Lagourette *et al.*, 1992; Holcomb & Outcalt, 1998; Bouchot, & Richon, 2001)

Metrological traceability of certified value shall be established in compliance with the requirements of ISO 17025 (2017). The certified values of density should be related to the SI measurement units of mass and length through a documented unbroken chain of calibrations.

2.4.2 Refractive index

The refractive index, n, of a solution is influenced by its composition, concentration, temperature, and the wavelength of incident light. This connection between solution concentration and refractive index finds applications, notably in measuring salt concentration. Determining the solution's refractive index involves utilizing the Snell-Descartes law, which links

the refractive index to the angle of propagation (as shown in Fig.2-4). And so, the metrological traceability of this method is given by its relation to the length unit.

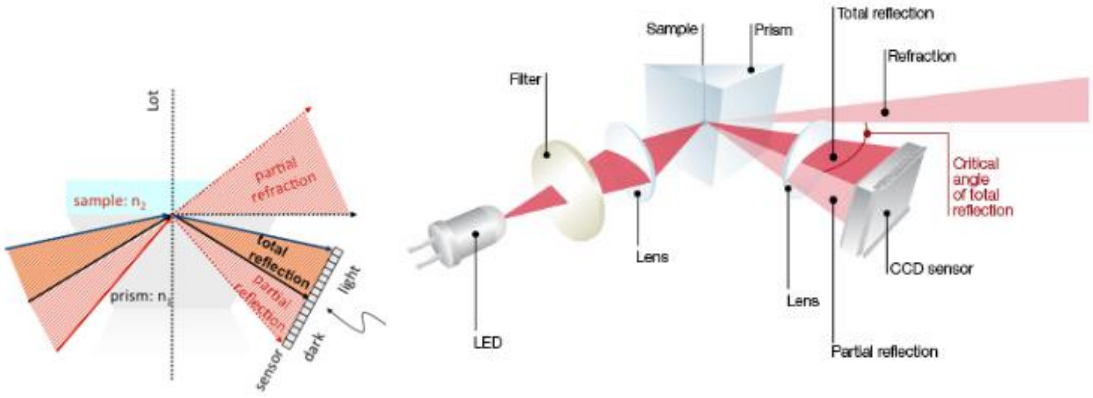

Figure 2-4 Schematics setup of a refractometer

(Anton Paar, 2023)

2.4.3 Speed of sound

Much like all waves, sound waves possess specific characteristics such as speed, frequency, and wavelength. A clear demonstration of sound's finite speed can be witnessed during a fireworks display. As the flash is observed long before the sound is heard. This phenomenon underscores the fact that sound travels at a finite rate, distinctly slower than light

This distinction in speed between light and sound becomes evident during a thunderstorm as well. A well-known way to estimate the distance of the lightning source is by counting the seconds between the flash and the sound. The velocity of any wave is intricately linked to its frequency and wavelength, as described by Eq. 2.6:

$$v = f\lambda \qquad \text{(Eq.2.6)}$$

Where:

v is the wave's speed;

f is the waves' frequency;

λ is the waves' wavelength.

The wavelength signifies the distance between consecutive identical points along the wave's profile. In the case of sound waves, this corresponds to the spacing between sequential compressions.

The frequency of a sound wave remains consistent with that of its source and signifies the number of wave cycles passing a specific point within a unit of time. Speed of sound varies

considerably across different mediums, this is contingent upon how rapidly vibrational energy can traverse through a given medium. Consequently, deriving the speed of sound in any particular medium hinges upon the inherent properties and conditions of that medium. In general, the formula for the speed of a mechanical wave in a medium relates to the square root of the medium's restorative force, F_R, divided by the inertial property, μ, as is shown in (Eq. 2.7).

$$v = \sqrt{\frac{F_R}{\mu}} \quad \text{(Eq.2.7)}$$

It is also important to note that the speed of a wave on a string is described by, (Eq. 2.8):

$$v = \sqrt{\frac{T}{\mu}} \quad \text{(Eq.2.8)}$$

Where:

T is the tension in the string;

μ is the inertial property.

Where the restoring force is the tension in the string T and the linear density μ is the inertial property. In a fluid, the speed of sound depends on the bulk modulus and the density, as Is described by, (Eq. 2.9) (California state university):

$$v = \sqrt{\frac{B}{\rho}} \quad \text{(Eq.2.9)}$$

Where:

B is the bulk modulus.

The two most used methods for measuring the speed of sound in seawater are the Acoustic Travel Time Method and the Acoustic Doppler Current Profiler. The Acoustic Travel Time Method is a straightforward method for measuring the speed of sound in seawater. This method involves measuring the time it takes for a sound wave to travel a known distance through seawater, i.e., time of flight (T_{Flight} in s) (Eq. 2.10). T_{Flight} can be determined using two acoustic transmitters placed at a known distance apart, L_0. The transmitter emits a sound pulse, and the time it takes for the pulse to travel from one transducer to the other is measured. By dividing the distance between the transmitters by the T_{Flight} of the sound pulse, the speed of sound, c in seawater can be calculated (Eq. 2.10).

$$c = \frac{L_0 \cdot f_1}{T_{\text{Flight}} - f_2} \quad \text{(Eq.2.10)}$$

Where:

f_1 is the correction factor for the change of path length caused by temperature variation Δt is the temperature deviation from 20 °C;

f_2 is the correction term for electronic delay, temperature, and dispersion/diffraction effects.

This means that the metrological traceability of the measurement result by this method is given by its relation to the time and length units.

The Acoustic Doppler Current Profiler (ADCP) is a more advanced method for measuring the speed of sound in seawater. This instrument uses the Doppler shift of sound waves to measure ocean currents and can also be used to measure the speed of sound in seawater. The ADCP emits a sound pulse at a known frequency, which is scattered back by particles in the water. By measuring the frequency shift of the returned signal, the speed of sound can be calculated. The ADCP can also provide information on ocean currents and water velocities, making it a valuable tool for oceanographic research.

2.4.3.1 Speed of Sound Equations

There are several equations that can be used to determine the speed of sound in samples of seawater based on the values of salinity, temperature, and pressure. Among these, the present study focuses on two equations whose range of validity covers the salinity range of the samples under study (Table 2-1). These equations are the Coppens (1981) equation and the UNESCO equation (Chen & Millero, 1977).

Table 2-1-Range of validity of Coppens and UNESCO equations

Equation	Temperature, T/ °C	Salinity, S / (g·kg^{-1})	Pressure, P / kPa	Depth, D / m
Coppens	[0, 35]	[0, 45]	-	[0, 4000]
UNESCO	[0, 40]	[0, 40]	[0, 10 0000]	-

2.4.3.1.1 Coppens

The Coppens' equation is given by the following set of equations, (Eq. 2.10-2.11.) (NPL):

$$c(D,S,t) = c(0,S,t) + (16.23 + 0.253t)D + (0.213 - 0{,}1t)D^2 + (0.016 + 0.0002(S-35))(S-35)tD$$
(Eq.2.10)

$$c(0,S,t) = 1449{,}05 + 45{,}7t - 5{,}21t^2 + 0{,}23t^3 + (1{,}333 - 0{,}126t + 0{,}009t^2)(S-35) \quad \text{(Eq.2.11)}$$

Where:

$t = \frac{T}{10}$ where T is temperature in ºC;

S is the salinity in g kg^{-1};

D is the depth in km.

With this equation, it is possible to compute speed of sound values with an associated expanded uncertainty of 0.1 m s^{-1} (Coppens, 1981).

2.4.3.1.2 The UNESCO equation: Chen and Millero

The UNESCO algorithm, also known as the international standard algorithm, was formulated by Chen and Millero back in 1977. In contrast to the simpler equations discussed later in this text, the UNESCO algorithm has a more intricate structure, as it factors in pressure as a variable rather than depth. For a comprehensive exploration of the original UNESCO algorithm, one should consult the research conducted by Fofonoff and Millard in 1983. In 1995, Wong and Zhu recalibrated the coefficients within this algorithm to align with the adoption of the International Temperature Scale of 1990. Their version of the UNESCO equation is presented as follows, (Eq. 2.12-2.16).

$$c(S,T,P) = Cw(T,P) + A(T,P)S + B(T,P)S^{\frac{3}{2}} + D(T,P)S^2 \quad \text{(Eq.2.12)}$$

$$Cw(T,P) = (C_{00} + C01T + C_{02}T^2 + C_{03}T^3 + C_{04}T^4 + C_{05}T^5) + (C_{10} + C_{11}T + C_{12}T^2 + C_{13}T^3 + C_{14}T^4)P + (C_{20} + C_{21}T + C_{22}T^2 + C_{23}T^3 + C_{24}T4)P2 + (C_{30} + C_{31}T + C_{32}T^2)P3 \quad \text{(Eq.2.13)}$$

$$A(T,P) = (A_{00} + A_{01}T + A_{02}T^2 + A_{03}T^3 + A_{04}T^4) + (A_{10} + A_{11}T + A_{12}T^2 + A_{13}T^3 + A_{14}T4)P + (A_{20} + A_{21}T + A_{22}T^2 + A_{23}T^3)P^2 + (A_{30} + A_{31}T + A_{32}T^2)P^3 \quad \text{(Eq.2.14)}$$

$$B(T,P) = B_{00} + B_{01}T + (B_{10} + B_{11}T)P \quad \text{(Eq.2.15)}$$

$$D(T,P) = D_{00} + D_{10}P \quad \text{(Eq.2.16)}$$

Where:

T is the temperature in ^{o}C;

S is the salinity in Practical Salinity Units (in g kg^{-1});

P is the pressure in bar.

The speed of sound values computed by UNESCO equation have an associated expanded uncertainty of 0.05 m s^{-1} (Allen, *et al.*, 2017).

2.5 Measurement Uncertainty

When disclosing the outcome of a measurement involving a physical quantity, it is imperative to provide a quantitative indication of the quality of this result. Only with such information can measurements be compared, both among themselves and against reference values specified by standards. The term "uncertainty" denotes doubt, and in its broader context,

"measurement uncertainty" refers to doubts surrounding the validity of a measurement result. Due to lexical limitations, "uncertainty" is used interchangeably for both the general concept of uncertainty and specific quantities that offer quantitative measures of the concept.

The formal definition of "measurement uncertainty" is the parameter characterizing the dispersion of the values being attributed to a measurand, based on the information used (VIM,2012).

The uncertainty of a measurement result reflects the lack of knowledge regarding the exact value of a measurand. Even after rectifying acknowledged systematic effects, the measurement result remains an estimation of the measurand's value, owing to the uncertainty tied to random effects and imperfect correction of systematic effects. It is worth noting that a measurement result, even after correction, can be very close to the measurand's value and still exhibit high uncertainty (BIPM, 2008).

In practical scenarios, numerous sources contribute to the uncertainty in a measurement, including: incomplete definition of the measurand; non-representative sampling of the measurand; inadequate understanding of the effects of environmental conditions on the measurand; and imperfect measurement of environmental conditions, among others. The standard uncertainty, u, quantifies the uncertainty of a measurement result and is expressed as a standard deviation.

Components of uncertainty can be categorized as Type A and Type B. These classifications are used to assess uncertainty components in two distinct manners, and they do not indicate the nature of the components. Both classifications rely on probability distributions, with resulting components quantified by variances or standard deviations. However, this classification isn't definitive, as uncertainty arising from the correction of a known systematic effect can be assessed using either Type A or Type B evaluation.

Type A uncertainties evaluation is performed through statistical analysis of a series of observations. A Type A standard uncertainty is derived from the probability density function, which is deduced from the observed frequency distribution. The (Eq. 2.7) allows to calculate the standard deviation of n independent observations. The standard uncertainty, $u(x_i)$, is given by the experimental standard deviation, s (Eq. 2.7) of the mean given in (Eq. 2.8).

$$s = \sqrt{\frac{1}{n-1}\sum_{j=1}^{n}(x_j - \bar{x})^2} \quad \text{(Eq.2.7)}$$

$$u(x_i) = \frac{s}{\sqrt{n}} \quad \text{(Eq.2.8)}$$

Where:

n is the number of independent observations;

x_j are the individually observed values;

$\bar{x}$ is the arithmetic mean of the individually observed values.

Type B evaluations, on the other hand, uses methods other than statistical analysis of observations. A Type B standard evaluation is derived from a presumed probability density function, based on the confidence level of an event occurring.

For uncorrelated input quantities, the square of the standard uncertainty of the output quantity estimate, y, is given by (Eq. 2.9.) The quantity $u_i(y)$ (i = 1, 2, ... , n) is the contribution to the standard uncertainty associated with the estimate of output quantity y, which results from the standard uncertainty associated with the estimate of input quantity, xi, as is shown in (Eq.2.10).

$$u^2(y) = \sum_{i=1}^{N} u_i^2(y) \quad \text{(Eq.2.9)}$$

$$u_i(y) = c_i \cdot u(x_i) \quad \text{(Eq.2.10)}$$

In equation II.10, c_i is the coefficient of sensitivity associated with the estimate of the input quantity x_i, i.e., $c_i(y(x_i)) = \left(\frac{\partial y}{\partial x_i}\right)$.

The combined standard uncertainty, $u_c(y)$, represents the uncertainty of a measurement result when the result is obtained from various other quantities. It is the estimated standard deviation associated with the result and is equal to the positive square root of the combined variance, obtained from all variance and covariance components of the involved quantities, regardless of their evaluation type (Eq. 2.11).

$$u_i(y(x_1, \dots, x_n)) = \sqrt{\sum_{i=1,n} \left(\frac{\partial y}{\partial x_i}\right)_i^2 u(x_i)^2 + 2 \sum_{i=1,n-1} \sum_{j=i+1,n} \left(\left(\frac{\partial y}{\partial x_i}\right) \left(\frac{\partial y}{\partial x_j}\right) \times cov(x_{ij}) \right)}$$

(Eq.2.11)

For the determination of the combined standard uncertainty of the mensurand, $u_c(\dots)$, the value of the square root of the variance, $u_c^2(x)$, of the influence quantities is estimated. For this purpose, it is considered that there is no correlation between the variables, and the equation of propagation of the uncertainties can be used in a simpler form, meaning the combined uncertainty, $u_c^2(y)$ is estimated via (Eq. 2.12).

$$u_c^2(y) = \sum_1^n \frac{\delta z}{\delta y_i}(y_1) \quad \text{(Eq.2.12)}$$

Were:

$u_c^2(y)$ is the standard uncertainty of the measurand;

y_1 , $\frac{\delta z}{\delta y_i}$ are the sensitivity coefficients that are derived from the calculation algorithm.

The number of effective degrees of freedom is calculated using the Welch-Satherwaite formula (Eq. 2.13).

$$\nu_{ef} = \frac{u^4(y)}{\sum_{i=1}^{N} \frac{u_i{}^4(y)}{\nu_i}} \text{ where } u_i(y) \ (i = 1, 2, ..., N) \quad \text{(Eq.2.13)}$$

For specific applications, an expanded uncertainty, U, is necessary. It defines the interval around the measurement result that is expected to encompass a significant portion of the distribution of values reasonably attributed to the measurand.

The expanded uncertainty is calculated by multiplying the combined standard uncertainty, $u_c(y)$, by an expansion factor, k (Eq. 2.14). The choice of the expansion factor, k, typically falls between 2 and 3 and is based on the associated confidence level of the interval. The expansion factor must always be provided to enable recovery of the standard uncertainty of the measured quantity.

$$U = k \cdot u_c(y) \quad \text{(Eq.2.14)}$$

Where:

U is the expanded uncertainty;

$u_c(y)$ is the combined standard uncertainty;

k is the expansion factor.

When all quantities upon which a measurement result depends are varied, their uncertainty can be assessed statistically. However, given practical constraints on time and resources, the uncertainty of a measurement is often evaluated using a mathematical model of the measurement and the law of uncertainty propagation. In some cases, the uncertainty of a correction for a systematic effect can be neglected in evaluating the uncertainty of a measurement result if its contribution to the combined uncertainty is insignificant. If the correction value itself is insignificant compared to the standard uncertainty, it too can be disregarded.

In essence, measurement uncertainty accounts for the variability and doubt inherent in measurement results. Through a systematic evaluation of various sources of uncertainty, both of Type A and Type B evaluations, the scientific community strives to ensure that measurement outcomes are presented in a way that accurately reflects their true quality and reliability.

2.6 Portuguese Institute for Quality

The Portuguese Institute for Quality (IPQ) is a public institution established in 1986 with a clear mission: to ensure the pursuit of quality in products and services, thereby enhancing the quality of life for citizens and boosting economic competitiveness within the context of increased freedom of goods circulation. IPQ holds a pivotal position in the landscape of Portuguese quality assurance, playing multiple crucial roles and functions. At the heart of IPQ's mission is the coordination of the Portuguese Quality System (SPQ) and other regulatory qualification systems as mandated by law. The institute actively promotes and coordinates activities that underpin the credibility of economic agents' actions, while also serving as the national metrology laboratory to ensure precision and accuracy in measurements.

More than an institution, IPQ stands as the national standardization organization and the institution responsible for metrology at a national level. It takes on the task of coordinating the Subsystem of Standardization, fostering and supporting the development of credible and sustainable national normative activities. Similarly, IPQ oversees the coordination of the system of Metrology, a responsibility that involves ensuring the accuracy, comparability, and traceability of measurements not only within Portugal but also on an international scale.

IPQ's vision extends beyond its roles, envisioning the Portuguese Quality System as a cornerstone for quality advancement across all sectors of activity within Portugal. This comprehensive vision seeks to drive greater productivity and national competitiveness, elevate the quality of life for citizens, and foster a culture steeped in quality consciousness. (IPQ,a, 2023)

2.6.1 Laboratory of Liquids Properties

The Laboratory of Liquids Properties (LPL) exists within the framework of the National Metrology Laboratory (NML) in the Department of Metrology (DMET) at IPQ, holding a vital role in the realm of metrology. LPL is entrusted with the responsibility of establishing and maintaining the national standards for key liquid properties, including mass density, viscosity, and surface tension of liquids.

Operating under the umbrella of IPQ's NML, the LPL plays a pivotal role in shaping the precision and reliability of liquid properties measurements. One of its primary functions is to prepare and certify reference materials for these fundamental properties. This entails developing measurement methodologies, conducting measurement audits, and calibrating equipment such as hydrometers, oscillation-type density meters, viscometers, rheometers, and tensiometers. Additionally, LPL undertakes a spectrum of activities, including tests within the

realm of Legal Metrology, training initiatives, and active participation in both national and international research and development projects.

The LPL's scope of operation is divided into three distinct areas, each addressing specific aspects of liquid properties:

- Surface Tension:

Within this area, the LPL focuses on understanding and quantifying the surface tension of liquids—a critical parameter with far-reaching implications in various industries, including pharmaceuticals, chemical processing, and material science.

- Viscosity:

The LPL's expertise in viscosity covers both dynamic and kinematic viscosity. Dynamic viscosity relates to the resistance of fluids to flow, while kinematic viscosity considers the fluid's flow characteristics relative to its density. This area's significance spans industries where fluid behavior and flow rates play a pivotal role.

- Mass Density:

The domain of mass density encompasses several subcategories, including hydrometry, oscillation tube densimetry, and hydrostatic weighing. These facets are integral to accurate measurements and formulations across a range of liquids, from simple solvents to complex chemical compositions.

The LPL's contributions extend beyond maintaining standards; it actively contributes to the advancement of metrology on national and international fronts. This is achieved through collaboration with partners across various sectors and the initiation of research endeavors that not only expand the boundaries of knowledge but also improve the precision of liquid property measurements. LPL's participation in training initiatives and engagement in research projects reinforces its commitment to the highest standards of quality in liquid property metrology. (IPQ, b, 2023)

2.6.2 Laboratory of Photometry, Radiometry and Radiofrequencies

Like LPL, the Laboratory of Photometry, Radiometry and Radiofrequencies (LFR) also operates under the umbrella of the NML in the DMET at IPQ. This laboratory's responsibilities encompass not only the tangible aspects of measurement but also the development and implementation of new methods and measurement capabilities. Through these endeavors, it ensures the traceability of its assigned units, enabling their widespread adoption at the national level. Collaborating on research and development projects, as well as interlaboratory comparisons, showcases the laboratory's dedication to pushing the boundaries of metrological

knowledge. Additionally, the laboratory provides essential support to legal metrology, ensuring that measurement standards align with regulatory requirements.

With a mission deeply rooted in the materialization, maintenance, and dissemination of units of measurement—ranging from luminous intensity and illuminance to reflection factors and refractive indices—the laboratory plays a critical role in fostering accuracy and consistency across diverse domains of measurement.

Within its sphere of activity, the LFR focuses on several key areas, each contributing to a robust and comprehensive metrological framework. Recognized internationally, these domains of expertise include:

- Luminous Intensity and Illuminance:

From luminous intensity ranging from 5 cd to 1000 cd to illuminance spanning from 5 lx to 1000 lx, this domain addresses the very essence of light perception and its quantification. Ensuring accurate measurement in these domains is crucial for fields ranging from lighting design to visual perception studies.

- Refractive Indices and Solution Properties:

The laboratory delves into the characterization of refractive indices in liquid solutions, covering a range from 1.332 98 to 1.720 000. Furthermore, the laboratory quantifies the mass fraction of saccharose or glucose in aqueous solutions up to 85.00 cg g^{-1} and the potential volume fraction of ethanol in aqueous solutions up to 55.00 cL L^{-1}. These capabilities hold significance across industries, including chemistry, pharmaceuticals, and food science.

- Speed Meter:

The laboratory's proficiency extends to measuring roadway speeds up to 350 km/h, providing essential data for transportation engineering and safety standards.

With international recognition on the horizon, the laboratory is in the advanced stages of securing acknowledgment for its proficiency in measuring regular transmission and reflection factors within the range from 0.01 to 0.90. Additionally, the laboratory is poised to delve into colorimetry (IPQ, c, 2023).

2.7 Measurement of Physical Properties of Salt Aqueous Solutions

Several studies have been performed by Furtado *et al*. (2010 and 2013) and Pellegrino *et al*. (2011a and 2011b) to investigate the metrological compatibility of the mass fraction results of some compounds, namely sodium chloride in aqueous solutions obtained by two different measuring techniques: refractometry and densimetry.

By definition, metrological compatibility is a property of a set of measurement results for a specified measurand, such that the absolute value of the difference of any pair of measured quantity values from two different measurement results is smaller than some chosen multiple of the standard measurement uncertainty of that difference. Indeed, the assignment of metrological compatibility to the measurement results, as defined in the International Vocabulary of Metrology, VIM (JCGM 2012), enables to decide whether the measurement results refer to the same measurand, when obtained by different measuring instruments, which would then be commutable.

In these studies, two measuring instruments were used: one digital refractometer Abbermar 550 from Anton Paar and one oscillation-type density meter (a DMA 5000 from Anton Paar). Particularly, in the most recent study, Furtado *et al*. (2022), prepared, by weighing, a set of sodium chloride aqueous solutions with an absolute salinity, S_A, within the interval [35; 215] g kg^{-1}. The main result of this work (Furtado *et al*., 2022) was to evidence metrological compatibility in salinity interval under study. Indeed, whatever the kind of NaCl aqueous solution or standard seawater sample (OSIL and ERM), the salinity measurement uncertainties are very similar, even though, low salinity values favour measurement dispersion. These results allow one to conclude that, in cases where matrix effects are expected, the use of the densimetry technique through the oscillation-tube density meter should be chosen. However, in the other cases, it is better to use refractometry, because it is a fast and cheap technique, which proved to provide salinity measurement results metrologically compatible with the previous one. Due to the observed greater dispersion of the experimental values at the lower bound of the salinity interval in this former work (Furtado *et al*., 2022), the aim of the present work is to extend the study of the metrological compatibility of density and refractive index measurement for the determination of smaller absolute salinity values within the [5; 40] g kg^{-1} interval . It is also an objective of this work, to validate the density measurement indications of a recent commercial oscillation-type density meter (DSA 5000M, Anton Paar), whose working principle is slightly different from DMA 5000 (Anton Paar), which was used and described in previously published studies (Furtado *et al*., 2010, 2013, 2022 and Pellegrino *et al*., 2011a, 2011b).

For both DSA 5000M and DMA 500 (Anton Paar) density meters, the sample is introduced into a U-shaped tube made of borosilicate glass that is being excited to oscillate at its characteristic frequency, which changes with temperature and density of the sample.

The difference from the previous model, is that after having reached a stable oscillation, the excitation is switched off, and the oscillation fades out, whereas for DMA 5000, the measuring cell maintains the oscillation throughout the entire measurement. In DSA 5000M

the excitation and fade-out sequence is repeated continuously. This patented "Pulsed Excitation Method" (AT 516420 (B1)) allows the instrument to determine the quality factor of the oscillating U-tube in a way that provides deeper insights into the sample's characteristics compared to any other oscillating U-tube method. The manufacturer claims that the "Pulsed Excitation Method" provides a better viscosity correction and a better repeatability of density results. Through continuous monitoring of the oscillation pattern during excitation and fade-out, followed by a mathematical conversion, the density of the sample can be measured. The density, ρ,is calculated from the quotient of oscillation periods, ρ, of the U-tube and the reference oscillator (Eq. 2. 15).

$$\rho = A \cdot \tau Q^2 \cdot f_1 - B \cdot f_2 \quad \text{(Eq.2.15)}$$

Where:

ρ is the density;

A and *B* are instrument specific coefficients, which are physically meaningful parameters of the oscillator determined by calibration fluids with at least 2 fluids;

Q is the oscillation period of the U-tube divided by the oscillation period of the reference oscillator;

f_1, f_2 are the correction factors for temperature, viscosity, and nonlinearity.

One of the goals of this work is to validate IPQ's speed of sound measurement system (Anton Paar, DSA 5000M), within the [1255.0, 1500.0] m s^{-1} interval, at 20 ^{o}C, by comparing the obtained results with reference values.

3

MATERIALS AND METHODS

This chapter explains the experimental steps that were followed in order to complete this study.

It is divided into three experimental parts. The first part consisted in the validation of density and speed of sound measurement results obtained with a DSA 5000 M (Anton Paar).

The second part consisted of studying the metrological compatibility of absolute salinity values obtained by two different measurement techniques: refractometry and densimetry.

In a third part, with the aim of studying the matrix effect, i.e., the different saline compositions, on the determined absolute salinity and compare them to the ones in ultrapure water solutions, a set of samples of standard seawater (SSW) was tested.

3.1 Validation of DSA 5000 M (Anton Paar) density and speed of sound

The validation of DSA 5000 M (Anton Paar) for density and speed of sound measurement results was performed as described in the points below.

3.1.1 Density calibration

The density interval of interest [1001.8, 1026.8] kg m^{-3} is the one corresponding to the absolute salinity interval under study of [5, 40] g kg^{-1}.

As none certified reference material (CRM) was available in this density interval, a set of NaCl (NaCl for analysis, ACS, ISO, PanReac Applichem ITW Reagents) aqueous solutions were prepared gravimetrically to obtain 8 solutions, by using a mass comparator of Mettler Toledo, PR 2004 (Fig. 3-1).

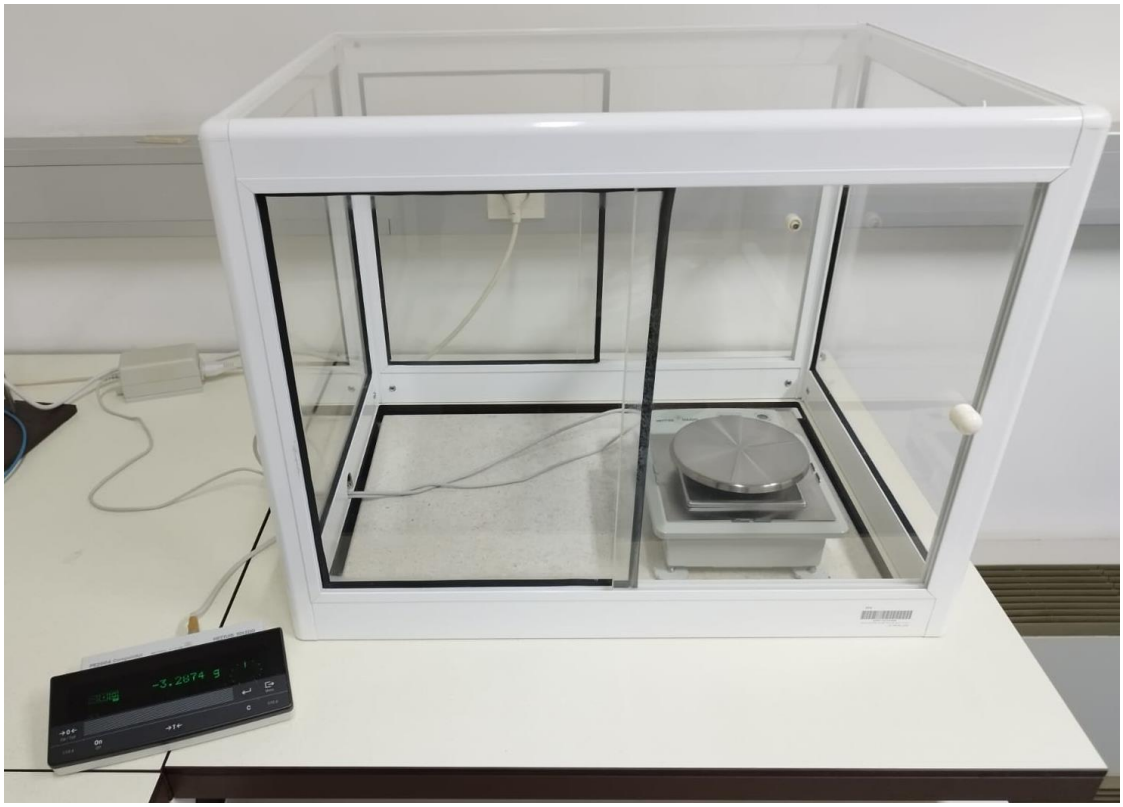

Figure 3-1 Mass comparator of Mettler Toledo

Ultrapure water (type I) (ISO 3696:1987) produced by the Milli Q Advantage water system (Merck Millipore) was used for the preparation of these solutions (Fig. 3-2).

Figure 3-2 Milli Q Advantage water system (Merck Millipore)

To ensure good homogeneity, all solutions were stirred for at least 60 min. The nominal values of mass fraction, X_m, density, ρ, dynamic viscosity, η, at 20 °C, of the NaCl solutions under test are summarized in Table 3-1.

Table 3-1 Nominal values of mass fraction, density, dynamic viscosity, at 20 °C

Samples codification	$S_{A,\,nom.}$ /(g kg^{-1})	ρ_{nom} /(kg m^{-3})	η_{nom} /(mPa s)	$X_{m,NaCL}$ /(cg g^{-1})
NaCl_5	5	1001.8	1.011	0.50
NaCl_10	10	1005.3	1.020	1.01
NaCl_15	15	1008.9	1.031	1.50
NaCl_20	20	1012.5	1.036	2.00
NaCl_25	25	1016.1	1.057	2.49
NaCl_30	30	1019.6	1.052	2.99
NaCl_35	35	1023.2	1.084	3.50
NaCl_40	40	1026.8	1.068	4.00

(Adapted from Wolf, 1996; Söhnel and Novotny, 1985)

The reference density values were obtained by measuring these solutions with a DMA 5000 (Anton Paar) density meter whose traceability of density measures to SI units is achieved by means of its calibration with CRM from National Metrology Institutes (GUM - Poland; NIST- USA and PTB - Germany) and by accredited laboratories (H&D Fitzgerald)

3.1.2 Temperature calibration

The SI traceability of temperature measurements performed by the DMA 5000 density meter is guaranteed by indirect thermometry using certified liquids for various temperatures and direct thermometry, by comparing the temperature indication of the density meter, with a 100 ohms platinum resistance thermometer (PRT) which was introduced into its measuring cell. This PRT was calibrated by the IPQ Temperature Laboratory.

For DSA 5000M, the temperature calibration was performed only by indirect thermometry using n-Dodecane, in the temperature interval from [10, 40] °C. The values from DMA 5000 were used as reference(Tables 3-2,3-3).

Table 3-2 Reference density values, and expanded uncertainties, of the reference liquids

Reference liquids	t / ºC	ρ / (kg m^{-3})	U_ρ / (kg m^{-3})	Source
n-Dodecane	10	756.042	0.016	DMA 5000 values
	15	752.414	0.018	
	20	748.788	0.001	
	25	745.155	0.018	
	30	741.524	0.018	
	35	737.887	0.019	
	40	734.246	0.018	

3.1.3 Viscosity damping and calibration

The error due to viscosity damping and the calibration of viscosity indication of DSA 5000M was performed with 8 reference liquids, produced, and certified in density and viscosity by Cannon. The reference liquids used cover the dynamic viscosity interval of [0.66; 500] mPa s.

Table 3-3 Reference values of density, dynamic viscosity, and respective expanded uncertainties

Samples codification	t / ºC	ρ / (kg m^{-3})	U_ρ / (kg m^{-3})	η / (mPa s)	U_η / (mPa s)	Metrological Traceability
N .8	20.000	866.29	0.050	0.66	0.0011	Cannon
N 1.0	20.000	729.95		0.92	0.0015	
N 2.0	20.000	759.67		2.085	0.0033	
N 4.0	20.000	787.39		5.53	0.0088	
N 14.0	20.000	812.20		23.70	0.052	
N 26.0	20.000	820.99		48.07	0.11	
N100	42.700	855.694		70.30	0.15	
	37.800	858.710		86.98	0.25	
	35.450	860.137		108.82	0.32	
	33.140	861.553		127.29	0.37	
	29.280	863.919		158.09	0.46	
	26.660	865.523		178.51	0.52	
S200	35.750	830.403		190.59	0.55	
	31.660	832.862		243	0.70	
N100	20.000	869.64		270.81	0.91	
S200	27.160	835.568		300.39	0.91	
	23.505	837.765		409.30	1.12	
	22.189	838.556		409.7	1.4	
	20.000	839.90		469.0	1.4	

3.1.4 Speed of sound calibration

As previously described, the speed of sound, c can be calculated by dividing the distance between the transmitters by the T_{Flight} of the sound pulse (Eq.3.1).

$$c = \frac{L_0 \cdot f_1}{\text{TFlight} - f_2} \quad \text{(Eq.3.1)}$$

Where:

c is the speed of sound

f_1 is the correction factor for the change of path length caused by temperature variation, for DSA 5000M this factor is given by $(1 + 1.6 \cdot 10^{-5} \cdot \Delta t)$, where Δt is the temperature deviation from 20 °C

f_2 Is the correction term for electronic delay, temperature, and dispersion/diffraction effects.

The speed of sound calibration of DSA 5000M (Anton Paar) was performed with 3 different liquids: degassed ultrapure water (ISO 3696:1987), n-Dodecane, and n-Decane, at 20 º C (Table 3-4). For ultrapure water the speed of sound indication values was compared with the ones given by Marczak (1997). For the remaining test liquids, the speed of sound reference values were consulted at NIST Chemistry Book on the Web (https://webbook.nist.gov/).

Table 3-4 Reference values of speed of sound, and respective uncertainty values

Reference liquids	t / °C	c_{ref} / (m s^{-1})	$U_{c_{ref}}$ / (m s^{-1})	Source
n-Decane	20	1253	13	(Lemmon & Span, 2006)*
n-Dodecane	20	1301.2	6.5	(Lemmon & Huber, 2004)*
Ultrapure water	20	1482.38	0.01	(Marczak, 1997)

As the main goal of this work is to validate the measurement of speed of sound in seawater, within the salinity range of 5 g kg^{-1} to 40 g kg^{-1}, corresponding to a speed of sound interval of around 1490 m s^{-1} to 1530 m s^{-1}, the DSA 5000M was also calibrated by means of 8 NaCl aqueous solutions, and 6 seawater dilutions made from OSIL SSW.

From the density measurement results of DSA 5000M the respective salinity values were determined by using the approach described at sub-chapter 3.2.3 (Eq. 3.7). The method of estimation of associated uncertainty values is presented at sub-chapter 3.2.4. With these salinity values the corresponding speed of sound values were determined by means of two reference equations: Coppens' equation (described in 2.4.3.1.1) and UNESCO equation (described 2.4.3.1.2). For calculations of sensitivity coefficients polynomial fits of S(c) were described as follows, for a temperature of 20 ºC for the 8 NaCl aqueous solutions:

$$S(c)_{\text{Coppens}} = -7.105427 \cdot 10^{-15}\, c^2 + 1.117000\, c + 1.482355 \cdot 10^3 \quad \text{(Eq.3.2)}$$

$$S(c)_{\text{UNESCO}} = 2.823288 \cdot 10^{-5} c^3 - 1.819477 \cdot 10^{-3} c^2 + 1.145433\, c + 1.482533 \cdot 10^3 \quad \text{(Eq.3.3)}$$

Given this approximation the sensitivity coefficients for speed of sound are the following: $\frac{\partial S(c)_{\text{Coppens}}}{\partial c} = 1.12$ and $\frac{\partial S(c)_{\text{UNESCO}}}{\partial c} = 1.14$.

For temperature the sensitivity coefficients were: $\frac{\partial S(c)_{\text{Coppens}}}{\partial t} = 1$ and $\frac{\partial S(c)_{\text{UNESCO}}}{\partial t} = 1$

And for a temperature of 20 ºC for the 6 seawater dilutions made from OSIL SSW:

$$S(c)_{\text{Coppens}} = -1.421085 \cdot 10^{-14} c^2 + 1{,}117000 c + 1{,}482355 \cdot 10^3 \quad \text{(Eq.3.4)}$$

$$S(c)_{\text{UNESCO}} = 2.145009 \cdot 10^{-5} c^3 - 1.624237 \cdot 10^{-3} c^2 + 1.148714 c + 1.482499 \cdot 10^3 \quad \text{(Eq.3.5)}$$

Given this approximation the sensitivity coefficients for speed of sound are the following: $\frac{\partial S(c)_{\text{Coppens}}}{\partial c} = 1.12$ and $\frac{\partial S(c)_{\text{UNESCO}}}{\partial c} = 1.15$. For temperature the sensitivity coefficients were 1: $\frac{\partial S(c)_{\text{Coppens}}}{\partial t} = 1$ and $\frac{\partial S(c)_{\text{UNESCO}}}{\partial t} = 1$

And so, the mathematical model used in both cases was:

$$c(S,T,P) = c_{\text{Coppens or UNESCO}} + \delta S + \delta T + \delta P + \delta c_{\text{Coppens or UNESCO}} \quad \text{II.6}$$

Where:

δS is the error due to the salinity determination via density measurements by using the approach described in subchapter 3.2.3. This error has zero average value but has a contribution value in uncertainty determined as described in subchapter 3.2.4;

δT is the error due to the temperature measurements. It was assumed that this error has zero average value but has a contribution value in uncertainty determined as described in subchapter 4.1.2;

δP is the error due to the pressure of the sample during measurements. It was assumed that this error has zero average value and a negligible contribution value in uncertainty as only low compressibility liquids were tested;

$\delta c_{\text{Coppens or UNESCO}}$ is the error due to the speed of sound obtained via Coppens (1981) or UNESCO (Allen, *et al.*, 2017) equations. This error has zero average value and contribution value in uncertainty 0.1 m s^{-1} and 0.05 m s^{-1}, respectively.

3.2 Salinity determination

The metrological compatibility of absolute salinity values, S_A obtained by refractometry and densimetry was investigated at 20 °C in the [5; 40] g kg^{-1} S_A interval, by using the same sodium chloride aqueous solutions from point 3.1.1 (Table 3-1).

The study of the matrix effect on absolute salinity determination was also undergone with a set of standard seawater (SSW) samples of two different sources, both with a nominal SA of 35 g kg^{-1}: OSIL (an open-ocean Atlantic Ocean water) and ERM (consists of an acidified coastal surface seawater) (Table 3-5).

Table 3-5 Nominal values of absolute salinity, of the seawater samples under test.

Samples codification	$S_{A,\,nom.}$ /(g kg^{-1})
SSW_OSIL_35	35
SSW_ERM_35	35

3.2.1 Density measurements

The density of the samples was measured with both density meters (DMA 5000 and DSA 5000M, from Anton Paar) (Fig. 3-3 and 3-4).

Figure 3-3 DMA 500 by Anton Paar

Figure 3-4 DSA 5000M by Anton Paar

3.2.2 Refractive index measurements

To measure the refractive indices of the samples, a refractometer Abbemat 550 by Anton Paar was employed (Fig. 3-5).

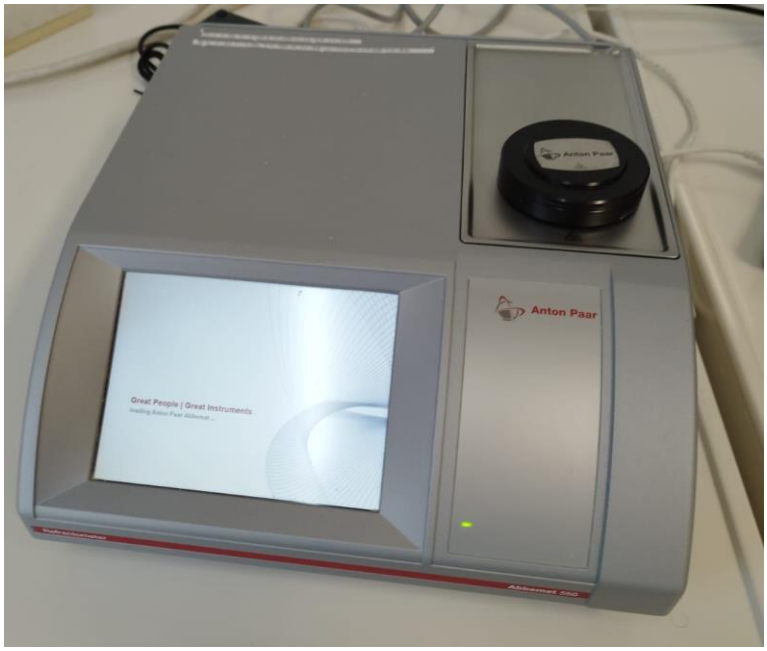

Figure 3-5 Abbemat 550 by Anton Paar

The measurements were taken within the range of [1.300 000; 1.720 000], and the instrument's accuracy was ensured through calibration using certified reference materials from renowned National Metrology Institutes (such as GUM in Poland, NIST in the USA, and PTB in Germany). This calibration process establishes a refractive index standard uncertainty of 0.000 010.

The critical angle in the Snell-Descartes law was determined using a charge-coupled device (CCD), which captured the refracted light after passing through the solution held in a small 0.4 mL cell. The experiment was conducted at a constant temperature of 20.00 °C, with illumination provided by a light-emitting diode (LED) emitting light at a wavelength of 589.3 nm.

3.2.3 From density and refractive index to salinity

The employed methodology to obtain the absolute salinity value of the test samples was like the one previously used (Furtado *et al.*, 2010, 2013, 2022 and Pellegrino *et al.*, 2011a, 2011b). Once the quantity of interest, the density, ρ , or the refractive index, n, was measured, internationally recognized reference tables were used to convert it into mass fraction, for the 20 ^{o}C reference temperature, as the quantities are temperature dependent. Linear interpolation in the intervals of the two successive tabled data are performed to deduce mass fraction value, as it provides a smaller uncertainty deduced value (Pellegrino *et al.*, 2009).

NaCl mass fractions were determined from density measurements, using density reference values published in 1985 by Söhnel & Novotny, whereas for refractive index measurements, the reference values were published in 1966 Wolf and that are still in use.
For instance, to obtain NaCl mass fraction value, $X_m(\rho)_p$ from the average between 5 and 7, N, density measurement values, at 20 ^{o}C, after correction based on certified reference materials (CRM), giving a density meter calibration function, with a C value according to:

$$\rho_p = \frac{\sum_{i=1}^{N} \rho_i}{N} + C \qquad \text{(Eq.3.7)}$$

An interpolation was done by using a set of pairs of values ($\rho_{(p\text{-}1)}$, $X_m(\rho)_{(p\text{-}1)}$) and ($\rho_{(p+1)}$, $X_m(\rho)_{(p+1)}$) from the reference values published by Söhnel and Novotny (1985), following:

$$X_m(\rho)_p = \frac{[\rho_p - \rho_{(p-1)}][X_m(\rho)_{(p-1)} - X_m(\rho)_{(p+1)}]}{\rho_{(p-1)} - \rho_{(p+1)}} + X_m(\rho)_{(p-1)} \qquad \text{(Eq.3.8)}$$

$$X_m(n)_p = \frac{[n_p\text{-}n_{(p\text{-}1)}][X_m(n)_{(p\text{-}1)}\text{-}X_m(n)_{(p+1)}]}{n_{(p\text{-}1)}\text{-}n_{(p+1)}} + X_m(n)_{(p\text{-}1)} \qquad \text{(Eq.3.9)}$$

From the interpolated value of the mass fraction in NaCl, $X_m(\rho)_p$, in cg g^{-1}, (Eq. 3.3), the value of absolute salinity was obtained by multiplication of a factor of 10, i.e. $S_A = 10\ X_m(\rho)_p$, in g kg^{-1}.

The same methodology was applied to refractive index values by using the refractometer calibration curve and the respective set of pairs of values from the reference values published by Wolf (1966).

3.2.4 Uncertainty budget of determination of the absolute salinity values

The uncertainty budget associated to the salinity was calculated and expressed within the Guide to the Expression of Uncertainty in Measurement - GUM (JCGM 100:2008) framework. The uncertainty associated with each input quantity is a combination of the three main sources: measurements repeatability, i.e., dispersion; the correction of the input value due to the temperature of the sample; and the component associated to the calibration of the measuring instruments (C). Concomitantly, the components of measurement uncertainty may be grouped into two categories, Type A and Type B, according to whether they were evaluated by statistical methods (Type A) or other methods (Type B). The uncertainty budget of the absolute salinity, SA, results obtained via density, S_A, results obtained via density, $S_A(\rho)$, and refractive index, $S_A(n)$, measurements at 20 ºC, is given on Table 3-6.

Table 3-6 Uncertainty budget of the absolute salinity results

Contribution	Measurement	Standard uncertainty	Method of evaluation	Distribution	Degrees of freedom
Instrument resolution	Density Refractive index	$\frac{10^{-3}}{\sqrt{12}}$ kg m^{-3} $\frac{10^{-6}}{\sqrt{12}}$	Type B	Rectangular	50
Instrument calibration (including drift)	Density Refractive index	10^{-2} kg m^{-3} 10^{-5}	Type B	Normal	50
Measurement repeatability	Density Refractive index	$\frac{\sigma}{\sqrt{N}}$	Type A	Normal	N-1
Temperature[1]	Density Refractive index	-	Type A	Normal	50
Interpolation (from ref. values[2,3])	Density Refractive index	6 10^{-3} kg m^{-3} 2 10^{-2}	Type B	Rectangular	50

Legend: σ – standard deviation of the N measurement values; 1 – the temperature uncertainty component is already taken into account in the uncertainty of the calibration of the measuring instrument; 2 – according to (Söhnel & Novotny, 1985), with a $U_\rho = (1\ 10^{-1})/(3)^{1/2}$ kg m^{-3}and $U_{Xm\mathrm{NaCl}} = (1\ 10^{-1})/(3)^{1/2}$ cg g^{-1} uncertainties; 3 – according to (Wolf, 1966), with a $U_n = (1\ 10^{-4})/(3)^{1/2}$ and $U_{Xm\mathrm{NaCl}} = (1\ 10^{-1})/(3)^{1/2}$ cg g^{-1} uncertainties.

4
RESULTS AND DISCUSSION

4.1 Validation of DSA 5000 M (Anton Paar) density and speed of sound meter

The validation of DSA 5000 M (Anton Paar) density and speed of sound measurement results are presented in the points below. According to the VIM 2.39, the calibration is an operation performed on a measurement system for given quantities. As the mesurand, is the density, depends on some quantities, the indication of which are given by the DSA 5000 M, the calibration of the latter for the quantities of interest is displayed in the following sections designated by the quantity in which the calibration is performed

4.1.1 Density calibration

In Table 4-1, are resumed the results obtained in DSA 5000 M density calibration. In this table are presented the density reference values, ρ_{ref} and respective uncertainties, $U_{\rho_{ref}}$ obtained with DMA 5000 density meter, and the density indication results of DSA 5000 M, without viscosity correction, d_{nc}, and with viscosity correction, d, and respective expanded uncertainties, $U_{d_{nc}}$ and U_d. The major contribution for the uncertainty of the reference value uncertainties, $U_{\rho_{ref}}$ is arising from DMA 5000 calibration uncertainty ($U_{\rho_{cal}}$= 0.020 kg m^{-3}), being the uncertainties contributions, the ones described in Table 4-1with exception of the uncertainty due to the interpolation. The uncertainties values of DSA 5000 M only took into consideration the uncertainty due to density resolution and due to measurement repeatability.

Table 4-1 DSA 5000 M density indications and DMA 5000 density reference values

Samples	DMA5000	DSA 5000M

codification	ρ_{ref}	$U_{\rho_{ref}}$	d_{nc}	$U_{d_{nc}}$	d	U_d
	/ (kg m^{-3})					
NaCl_5	1001.781	0.020	1001.775	0.001	1001.769	0.001
NaCl_10	1005.344	0.020	1005.340	0.001	1005.334	0.001
NaCl_15	1008.908	0.020	1008.902	0.001	1008.895	0.001
NaCl_20	1012.475	0.020	1012.478	0.001	1012.471	0.001
NaCl_25	1015.980	0.020	1015.973	0.001	1015.965	0.001
NaCl_30	1019.564	0.020	1019.564	0.002	1019.556	0.003
NaCl_35	1023.222	0.020	1023.229	0.001	1023.221	0.001
NaCl_40	1026.797	0.020	1026.791	0.001	1026.783	0.001

Table 4-2 summarizes DSA 5000 M density indication errors ($\delta d_{nc} = d_{nc} - \rho_{ref}$ and $\delta d = d - \rho_{ref}$) and respective expanded uncertainties ($U_{\delta d_{nc}} = \sqrt{{U_{\rho_{ref}}}^2 + {U_{d_{nc}}}^2}$ and $U_{\delta d} = \sqrt{{U_{\rho_{ref}}}^2 + {U_d}^2}$).

Table 4-2 DSA 5000 M density indication errors and respective expanded uncertainties

Samples codification	DSA 5000M			
	δd_{nc}	$U_{\delta d_{nc}}$	δd	$U_{\delta d}$
	/ (kg m^{-3})			
NaCl_5	-0.006	0.020	-0.012	0.020
NaCl_10	-0.004	0.020	-0.010	0.020
NaCl_15	-0.006	0.020	-0.013	0.020
NaCl_20	0.003	0.020	-0.005	0.020
NaCl_25	-0.007	0.020	-0.015	0.020
NaCl_30	0.001	0.020	-0.007	0.020
NaCl_35	0.008	0.020	-0.001	0.020
NaCl_40	-0.006	0.020	-0.014	0.020

From Figure 4-1, it is possible to observe that there is no relation between both density indication errors and density, and that the density indication errors are not meaningful as they are covered by the uncertainty, i.e., all the errors are smaller than 0.020 kg m^{-3}. This means that there is no need to apply any correction to density indication values. Interesting to note that density indication errors without viscosity correction, δd_{nc} were shown to be lower than the ones with viscosity correction, δd.

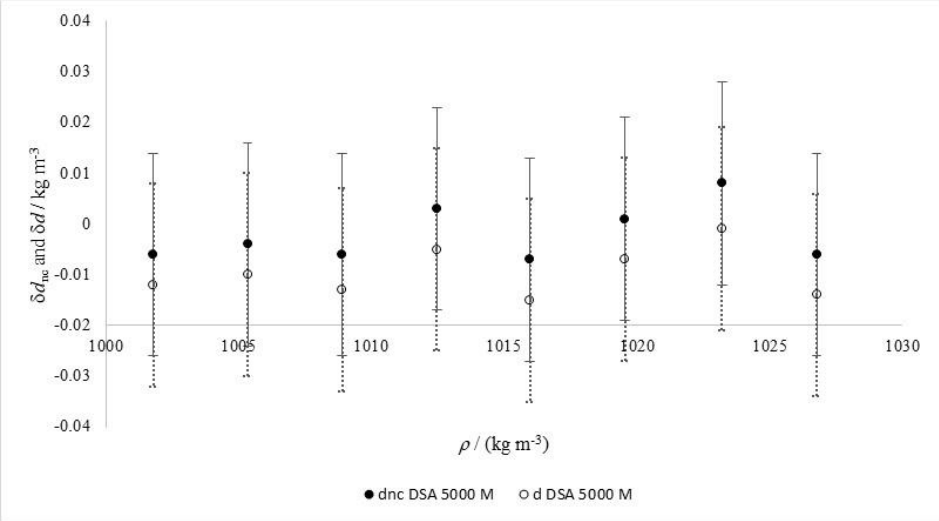

Figure 4-1 DSA 5000 M density indication errors and expanded uncertainties

4.1.2 Temperature calibration

DSA 5000M temperature calibration was performed by indirect thermometry by using n-Dodecane, in the temperature interval [10, 40] ºC. The results of this calibration are given in Table 4-3. From the reference density values given in Table 4-3 for n-Dodecane, a relation of t(ºC) was established to allow the calculation of temperatures values expected for the experimental density results. Using this approach, and from the results given in Table 10, a maximum temperature deviation was observed at 30 ºC, and a minimum at 10 ºC. From these results, a tolerance of 0.038 ºC will be added to the uncertainty budget of DSA 5000 M.

Table 4-3 DSA 5000 M density indication errors and respective expanded uncertainties

Reference liquids	DSA 5000M				
	t / ºC	δd_{nc}	$U_{\delta d_{nc}}$	δd	U_{δ_d}
		/ (kg m^{-3})			
n-Dodecane	10	0.015	0.024	0.001	0.024
	15	0.021	0.025	0.006	0.025
	20	0.023	0.021	0.004	0.021
	25	0.029	0.025	0.013	0.025
	30	0.029	0.025	0.016	0.025
	35	0.031	0.025	0.018	0.025
	40	0.029	0.025	0.017	0.025

Table 4-4 Resume of DSA 5000 M temperature indication errors

t	DSA5000 M	
	$\delta t(d_{nc})$	$\delta t(d)$

/ °C	/ °C	
10	0.007	-0.003
15	-0.006	-0.016
20	-0.013	-0.025
25	-0.024	-0.035
30	-0.029	-0.038
35	-0.026	-0.034
40	-0.012	-0.021

4.1.3 Viscosity calibration

The error due to viscosity damping and the calibration of viscosity indication of DSA 5000M was performed with 8 reference liquids from Cannon. The results are summarized in Tables 4-5 and 4-6 and represented in Figure 4-2. Both density indications errors have similar behavior with increasing viscosities, however, reaching plateaus at different viscosity values (around 180 mPa s for d_{nc} and around 70 mPa s for d). As expected, the density indication errors of d_{nc} are around 6-fold the ones of d. For d indications the error are considered neglectable below viscosities of around 70 mPa s as the uncertainty is higher than the deviation.

Table 4-5 DSA 5000 M density results and respective uncertainties

η / (mPa s)	d_{nc}	$U_{d_{nc}}$	d	U_d
	/ (kg m^{-3})			
0.656	866.306	0.050	866.309	0.050
0.920	729.950	0.050	729.943	0.050
2.085	759.679	0.050	759.654	0.050
5.525	787.471	0.050	787.401	0.050
23.700	812.341	0.050	812.155	0.050
48.069	821.260	0.050	820.980	0.050
70.321	856.121	0.052	855.767	0.052
90.859	859.197	0.052	858.799	0.052
103.470	860.655	0.052	860.234	0.052
118.298	862.101	0.052	861.650	0.052
149.135	864.519	0.052	864.031	0.052
175.120	866.156	0.052	865.641	0.052
187.305	830.987	0.050	830.468	0.050
226.656	833.396	0.050	832.846	0.050
233.202	833.701	0.050	833.147	0.050
237.559	869.081	0.050	868.525	0.050
240.053	834.006	0.050	833.449	0.050
245.556	869.393	0.050	868.833	0.050
247.212	834.311	0.050	833.752	0.050
253.762	869.706	0.050	869.142	0.050
254.677	834.616	0.050	834.054	0.050
262.175	870.017	0.050	869.449	0.050
262.451	834.920	0.050	834.355	0.050
270.531	835.227	0.050	834.660	0.050
270.806	870.324	0.050	869.750	0.050
302.899	836.229	0.050	835.652	0.050
379.842	838.457	0.050	837.866	0.050
411.451	839.261	0.050	838.666	0.050
469.000	840.579	0.050	839.979	0.050

Table 4-6 DSA 5000 M density errors and expanded uncertainties

η / (mPa s)	δd_{nc}	$U_{\delta d_{nc}}$	δd	$U_{\delta d}$
	/ (kg m^{-3})			
0.656	0.016	0.071	0.019	0.071
0.920	0.000	0.071	-0.007	0.071
2.085	0.009	0.071	-0.016	0.071
5.525	0.081	0.071	0.011	0.071
23.700	0.141	0.071	-0.045	0.071
48.069	0.270	0.071	-0.010	0.071
70.321	0.421	0.074	0.067	0.074
90.859	0.497	0.074	0.099	0.074
103.470	0.555	0.074	0.134	0.074
118.298	0.501	0.074	0.050	0.074
149.135	0.619	0.074	0.131	0.074
175.120	0.556	0.074	0.041	0.074
187.305	0.587	0.071	0.068	0.071
226.656	0.696	0.071	0.146	0.071
233.202	0.701	0.071	0.147	0.071
237.559	0.681	0.071	0.125	0.071
240.053	0.706	0.071	0.149	0.071
245.556	0.693	0.071	0.133	0.071
247.212	0.710	0.071	0.151	0.071
253.762	0.706	0.071	0.142	0.071
254.677	0.716	0.071	0.154	0.071
262.175	0.717	0.071	0.149	0.071
262.451	0.720	0.071	0.155	0.071
270.531	0.727	0.071	0.160	0.071
270.806	0.684	0.071	0.110	0.071
302.899	0.669	0.071	0.092	0.071
379.842	0.657	0.071	0.066	0.071
411.451	0.661	0.071	0.066	0.071
469.000	0.679	0.071	0.079	0.071

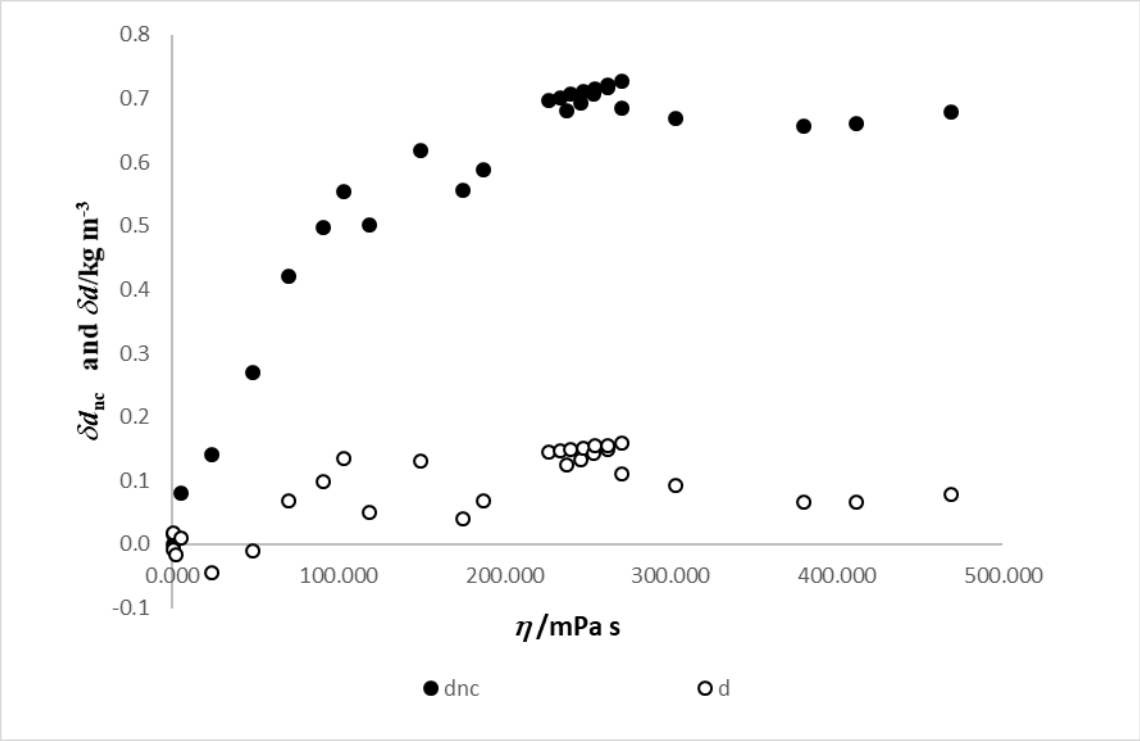

Figure 4-2 Density indication errors versus dynamic viscosity

4.1.3.1 DSA 5000M Calibration Curves

In previous studies (Furtado *et al.*, 2017) it was shown that the results of the difference between the density indication values not viscosity corrected, d_{nc}, and viscosity-corrected, d, for simplification denoted from now on as D, was studied using the same premises of the previous point. Density indication errors versus dynamic viscosity can be well described by polynomial regressions of third order for DMA 5000M (Anton Paar) density meters. With this relation it was possible to estimate the viscosity of the Newtonian liquids tested, in the viscosity interval from 7 mPa s to 220 mPa s, with a relative standard uncertainty of 3 %. Using the premises of this work, a relationship between dynamic viscosity with error of the density indication values not viscosity corrected, d_{nc}, and a relationship between D with error of the density indication values not viscosity corrected, d_{nc}. The same approach was used to estimate dynamic viscosity from obtained D values. Both, DMA 5000 and DSA 5000 M (Anton Paar) results were assessed using these approaches.

4.1.3.1.1 Calibration curve η versus δd_{nc}

In the first approach the data set was divided in two zones: the first one for the viscosity interval η of [0.65; 187] mPa.s and second for the viscosity interval η of [226; 469] mPa.s. A polynomial fit of third order was applied to the first set of data, Eq IV. 1 resulting in a maximum residual of 0.00055 g cm^{-3}. As can be seen in Figure 4-3, the linear fit of the second set of data (Eq. 4.2), corresponding to the viscosity interval of [226; 469] mPa.s, presents a weak correlation, with a determination factor R^2 of ~0.053. For this reason, the mean error value was determined showing a value 0.000697 g cm^{-3}.

$$\delta = -3.016139 \cdot 10^{-11} \cdot \eta^3 - 1.466820 \cdot 10^{-8} \cdot \eta^2 + 6.806690 \cdot 10^{-6} \cdot \eta + 6.409347 \cdot 10^{-6} \quad \text{(Eq.4.1)}$$

$$\delta = -1.096288 \cdot 10^{-7} \cdot \eta + 7.192490 \cdot 10^{-4} \quad \text{(Eq.4.2)}$$

Where:

δ is the indication error;

η is the dynamic viscosity.

The maximum residual obtained was 0.000040 g cm^{-3}. The uncertainty budget of each zone is presented in Table 4-7.

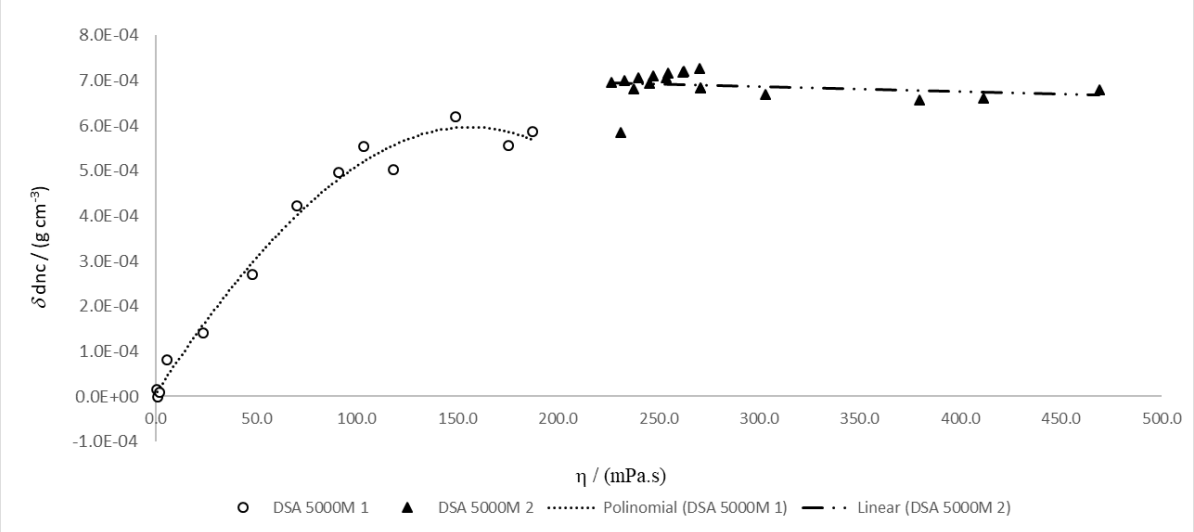

Figure 4-3 DSA 5000 M density indication errors versus dynamic viscosity

Table 4-7 Uncertainty budget of zone 1 and 2

	u crm	u max. res.	u_c	U (k=2,00, 95 %)
	g/cm³			
Zone 1	0.000025	-0.000032	0.000040	0.000081
Zone 2	0.000025	-0.000022	0.000034	0.000069

The main contributions for the final uncertainty are the following: the uncertainty of the certified reference material (CRM), including the standard-deviation obtained during the calibration and the uncertainty due to maximum residual (corresponding to a rectangular distribution calculated as the maximum residual (denominated as max. res. in Table 4-7) divided by the squared root of 3. In zone 2, the standard deviation of the mean error value is also considered. The expanded uncertainty of the interpolated values of first zone is 0.000081 g cm^{-3} and for the second zone, 0.000071 g cm^{-3}. However, to predict the correction within the interval of viscosities [187; 226] mPa s, due to lack of experimental data, two approaches were used: first a polynomial fit from zone 1 was used to predict the errors within this interval obtaining a residual of -0.000251 g cm^{-3} leading to an uncertainty of 0.000294 g cm^{-3}; and secondly, the mean density error of zone 2 was applied and a residual of 0.000110 g cm^{-3} was reached, leading to an uncertainty of 0.000138 g cm^{-3}.

In a second approach the entire set of data, with exception of two values considered as outliers, i.e., values which were inconsistent with other members of this set, was fitted with a third-degree polynomial equation (Eq. 4.3) shown in Figure 4-4, with a determination factor R^2 of ~0.993.

$$\delta = 2.308519 \cdot 10^{-11} \cdot \eta^3 - 2.274314 \cdot 10^{-8} \cdot \eta^2 + 7.025611 \cdot 10^{-7} \cdot \eta + 6.723188 \cdot 10^{-6} \quad \text{(Eq.4.3)}$$

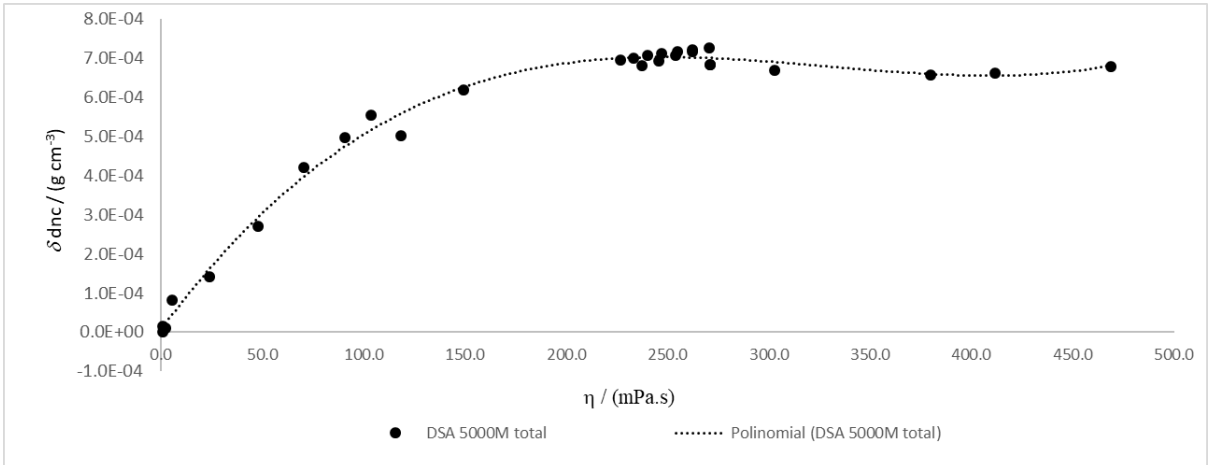

Figure 4-4 DSA 5000 M density indication errors versus dynamic viscosity

Despite several statistical assessment being available to be use for outliers confirmation (e.g., ISO 5725-2:1994), the simple approach of the maximum residual, i.e., the difference between the interpolated value and the obtained value, was used. From this the values obtained for nominal viscosities of 175 mPa s and 231 mPa s were considered outliers. The main contributions for the final uncertainty of this calibration curve are the same as previously described for zone 1, leading to an uncertainty value of 0.000082 g cm^{-3}, for k=2.00.

4.1.3.1.2 Calibration curve δd_{nc} versus D

Quite often the viscosity of liquid samples tested in this density meters are unknown, meaning that the calibration curve of δd_{nc} vs η is not useful. Earlier unpublished studies with DMA 5000 data, demonstrated that a calibration curve of δd_{nc} against D can be used in these cases with a relatively low uncertainty value.

Similarly, to what was done for the calibration curve δd_{nc} vs η, two approaches were applied. In the first approach the data set was divided in two zones: the first one for the D interval of [0; 0.000520] g cm^{-3}and second for the D 0.000550 g cm^{-3}. A polynomial fit of third order was applied to the first set of data (Eq. 4.4) resulting in a maximum residual of - 0.000050 g cm^{-3}. As can be seen in Figure 4-5, the linear fit of the second set of data (Eq. IV.5), for $D \geq 0.000550$ g cm^{-3}, presents a very weak correlation, with a determination factor R^2 of ~0.008. For this reason, the mean error value was determined with value of 0.000697 g cm^{-3}.

$$\delta = -8.070321 \cdot 10^{6} \cdot D^{3} + 6.789801 \cdot 10^{3} \cdot D^{2} - 2.526288 \cdot 10^{-1} \cdot D + 1.835188 \cdot 10^{-5} \quad \text{(Eq.4.4)}$$

$$\delta = -9.126431 \cdot 10^{-1} \cdot D + 1.213557 \cdot 10^{-3} \quad \text{(Eq.4.5)}$$

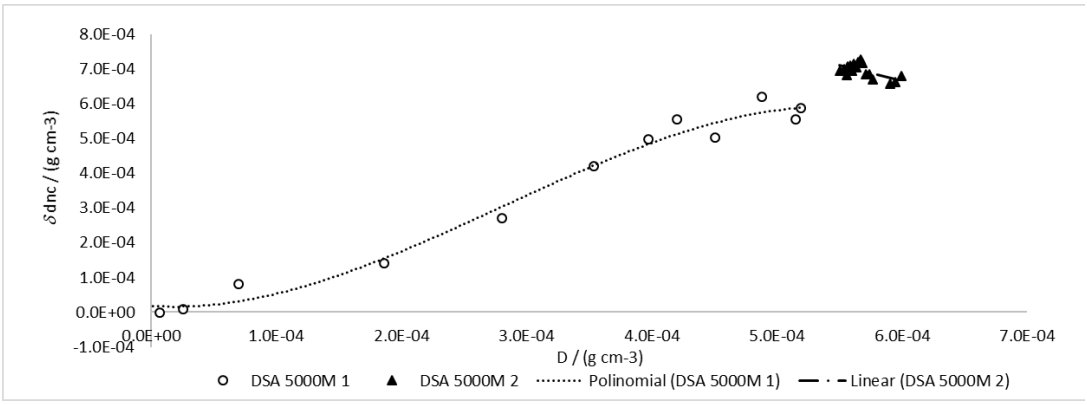

Figure 4-5 DSA 5000 M density indication errors versus *D*

The maximum residual obtained was 0.000040 g cm^{-3}. The uncertainty budget of each zone is presented in Table 4-8.

Table 4-8 uncertainty budget of zone 1 and 2

	u_{crm}	$u_{max.\ res.}$	u_c	U (k=2,00, 95 %)
	g/cm^3			
Zone 1	0.000 025	-0.000029	0.000038	0.000076
Zone 2	0.000 025	0.000022	0.000034	0.000069

The expanded uncertainty of the interpolated values of first zone is 0.000105 g cm^{-3}and for the second zone, 0.000178 g cm^{-3}. However, to predict the correction within D interval of [0.000520; 0.000550] g cm^{-3}, due to lack of experimental data, two approaches were used: first a polynomial fit from zone 1 was used to predict the errors within this interval obtaining a residual of -0.000 105 g cm^{-3} leading to an uncertainty of 0.000 178 g cm^{-3}; and secondly, the mean density error of zone 2 was applied and a residual of 0.000 040 g cm^{-3} was reached, leading to an uncertainty of 0.000 071 g cm^{-3}.

In a second approach the entire set of data, with exception of two values considered as outliers, i.e., values which were inconsistent with other members of this set, was fitted with a fourth-degree polynomial equation (Eq. 4.6), as shown in Figure 4-6 with a determination factor R^2 of ~0.991, with an uncertainty of 0.000105 g cm^{-3}, for k=2,00.

$$\delta = -2.526038 \cdot 10^{1} \cdot D^4 + 2.435898 \cdot 10^{7} \cdot D^3 - 5.605640 \cdot 10^{3} \cdot D^2 + 1.174382 \cdot D + 1.805745 \cdot 10^{-6} \quad \text{(Eq.4.6)}$$

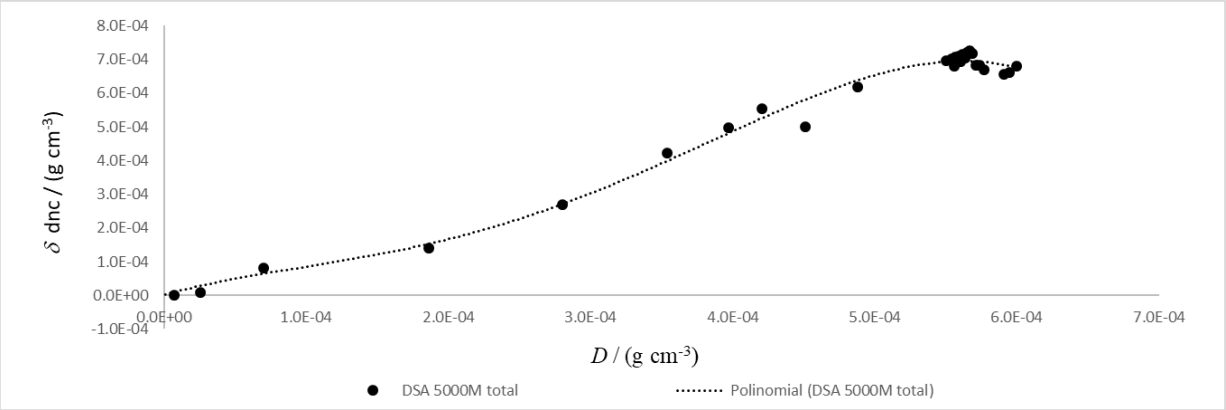

Figure 4-6 DSA 5000 M density indication errors versus *D*

4.1.3.2 Viscosity calibration curve

4.1.3.2.1 Viscosity estimation from D vs viscosity curve

With the calibration data, it was possible to establish two 3rd degree polynomial curves

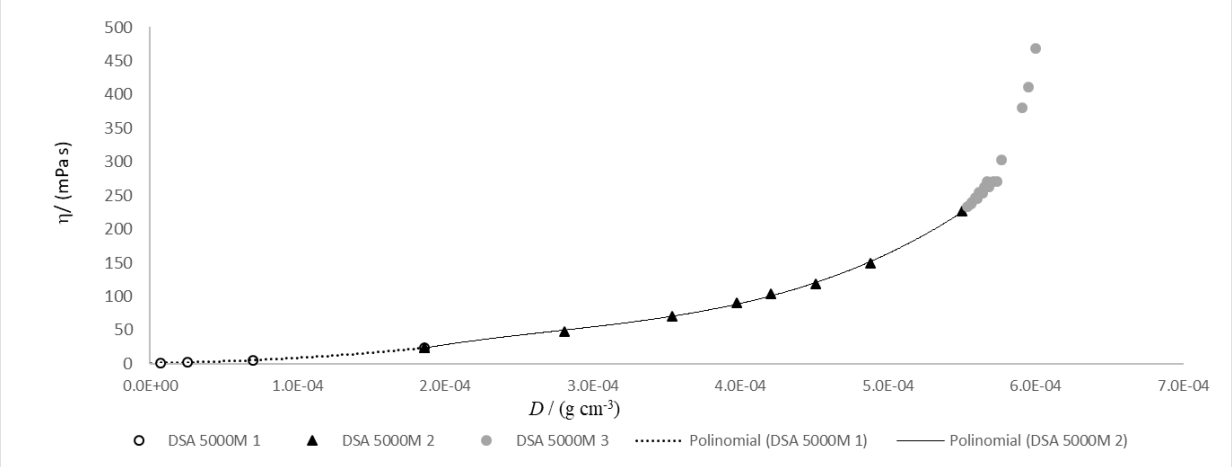

of η vs D (Eq.4.7 and 4.8). The first comprising the [0; 0.000186] g/cm³ D interval corresponding to the [0.65; 23.7] mPa s dynamic viscosity interval (Eq. 4.7), and the second comprising the]0.000186; 0.000550] g/cm³ D interval, corresponding to the]23.7; 227] mPa s dynamic viscosity interval (Eq. 4.8).

$$\eta = 5.040705 \cdot 10^{11} \cdot D^3 + 3.426962 \cdot 10^{8} \cdot D^2 + 4.240073 \cdot 10^{4} \cdot D + 7.135947 \cdot 10^{-1} \quad \text{(Eq.4.7)}$$

$$\eta = 5.142076 \cdot 10^{12} \cdot D^3 - 4.210034 \cdot 10^{9} \cdot D^2 + 1.393441 \cdot 10^{6} \cdot D - 1.231869 \cdot 10^{2} \quad \text{(Eq.4.8)}$$

With the first curve, from D, it is possible to estimate the dynamic viscosity value of the tested sample with a 12.7 % relative expanded uncertainty. The second curve gives a 4.5 % relative expanded uncertainty. When comparing with previous studies (Furtado *et al*., 2017), where a 3 %relative standard uncertainty was achieved for a [7, 220] mPa s viscosity interval, only the second interval displayed a relative uncertainty of the same magnitude. This fact may be justified with the use of CRM with higher uncertainty in DSA 5000 M. These two curves can be seen in Figure 4-7, for D values above 0.000583 g cm-3, the former assumptions are no longer valid.

4.1.3.3 Viscosity indication error

In this section, are displayed the results of the DSA 5000 M dynamic viscosity calibration, performed in the [23.7, 227] mPa s interval. The viscosity indication relative errors of DSA

Figure 4-7 DSA 5000 M Viscosity estimation from D versus dynamic viscosity

5000 M, $\delta\eta$, was calculated using as reference value the viscosity of CRM. The viscosity indication relative errors of DSA 5000 M determined by using the approach explained in the previous point, $\delta\eta$ polinomial curve, and respective relative uncertainty.

The viscosity indication relative errors, $\delta\eta$ DSA 5000 M, varied in absolute values between 0.47 % to 6.61 %, with a maximum expanded uncertainty of 1.2 %. The results of normalized error statistics, E_n, shown that the errors arising from this to calibration techniques are non-satisfactory, i.e., E_n >1, for viscosities of ~24 mPa.s, and from ~134 mPa.s to ~175 mPa.s. For this reason, maybe due to uncertainty underestimation.

4.1.4 Speed of sound calibration

In a first approach the calibration of DSA 5000M (Anton Paar) speed of sound indication was performed by using 3 different liquids: degassed ultrapure water, n-Dodecane and Decane at 20 °C. The resume of DSA 5000 M speed of sound indications, error δc, and uncertainty, $U\delta c$ obtained in the calibration are given in Table 4-9.

Table 4-9 DSA 5000 M speed of sound indications, error δ and uncertainty

Reference liquids	t / °C	c / (m s^{-1})	δc / (m s^{-1})	δ'c / %	$U\delta c$ / (m s^{-1})	$U\delta$'c / %
n-Decane	20	1255.0	2	0.2	25	2.0
n-Dodecane	20	1298.9	-2	-0.2	13	1.0
Ultrapure water	20	1483.9	1.5	0.1	4.5	0.3

The speed of sound indication errors can be considered neglectable (with a maximum relative error, δ'c of 0.2 %) as they are comprised within the uncertainty (with a maximum relative expanded uncertainty, $U\delta$'c of 2 %). For the future this uncertainty value will be used as tolerance.

The primary objective of this study is to verify the accuracy of measuring the speed of sound in seawater across a salinity interval of [5, 40] g kg^{-1}, corresponding to a speed of sound range of approximately [1490, 1530] m s^{-1}. In pursuit of this goal, we calibrated the DSA 5000M using 8 aqueous solutions of NaCl and 6 dilutions of seawater prepared from OSIL SSW. The reference values of speed of sound, c_{ref}, and respective uncertainty values, $U_{c_{ref}}$ of the NaCl aqueous solutions and OSIL aqueous solutions used as reference for the calibration of DSA 5000M are presented, in Tables 4-10 and 4-11, respectively.

Table 4-10 Reference values of speed of sound and respective uncertainty values

Source		$S_A(\rho)$ /(g kg^{-1})	$U_{SA(\rho)}$ /(g kg^{-1})	Coppens equation		UNESCO equation	
Reference liquids	t / °C			$c_{SA\ C\ (\rho)}$ / (m s^{-1})	$Uc_{SA\ C(\rho)}$ / (m s^{-1})	$c_{SA\ U\ (\rho)}$ / (m s^{-1})	$Uc_{SA\ U(\rho)}$ / (m s^{-1})
NaCl_5	20	5.0	1.2	1487.94	0.10	1488.23	0.05
NaCl_10	20	10.1	1.2	1493.64	0.10	1493.94	0.05
NaCl_15	20	15.0	0.8	1499.11	0.10	1499.39	0.05
NaCl_20	20	20.0	1.2	1504.70	0.10	1504.94	0.05
NaCl_25	20	24.9	0.8	1510.16	0.10	1510.39	0.05
NaCl_30	20	30.0	1.2	1515.83	0.10	1515.95	0.05
NaCl_35	20	35.0	0.8	1521.49	0.10	1521.65	0.05
NaCl_40	20	40.0	1.2	1527.04	0.10	1527.25	0.05

Table 4-11 Reference values of speed of sound, and respective uncertainty values

Source		$S_A(\rho)$ /(g kg^{-1})	$U_{SA(\rho)}$ /(g kg^{-1})	Coppens equation		UNESCO equation	
Reference liquids	t / °C			$c_{SA\ C\ (\rho)}$ / (m s^{-1})	$Uc_{SA\ C(\rho)}$ / (m s^{-1})	$c_{SA\ U\ (\rho)}$ / (m s^{-1})	$Uc_{SA\ U(\rho)}$ / (m s^{-1})
OSIL_5	20	5.1	1.1	1488.08	0.10	1488.34	0.05
OSIL_10	20	10.3	1.1	1493.82	0.10	1494.16	0.05
OSIL_15	20	15.3	0.8	1499.42	0.10	1499.72	0.05
OSIL_20	20	20.3	1.2	1504.98	0.10	1505.28	0.05
OSIL_25	20	25.2	0.8	1510.46	0.10	1510.72	0.05
OSIL_30	20	30.2	1.2	1516.08	0.10	1516.29	0.05

The results of the speed of sound in seawater measurements across a salinity range spanning from 5 to 40 g kg^{-1} at 20 °C, are given in Tables 4-12 and 4-13. The obtained results were assessed by means of the normalized error, E_n. The results were satisfactory, i.e., $E_n \leq 1$, in the entire salinity range, meaning that the measurement of speed of sound in seawater, within the salinity range of 5 to 40 g kg^{-1} is valid. It is important to state that $U\delta c_{\ DSA}$ is of greater magnitude due to the uncertainty associated with the conversion of density to practical salinity arising from the reference values (see subchapter 3.2.4). So, it is of relevance to note that relative errors obtained for both type of solutions (NaCl and OSIL aqueous solutions), and from both reference equations (Coppens, UNESCO) are $0.02\ \% \leq \delta' c \leq 0.42\ \%$. No trend seems to exist in what relates to relative errors $\delta' c$ and speed of sound results $c_{\ DSA}$, however the relative error of the NaCl aqueous solutions is always higher than the OSIL aqueous solutions as is shown in Figure 4-8. No further observations are made because the errors are comprised within the uncertainty.

Table 4-12 DSA 5000 M Speed of sound results and respective uncertainty values

Samples codification	c_{DSA}	Uc_{DSA}	Deviation from Coppens Eq.				En	Deviation from UNESCO Eq.				En
			δc	$U\delta c$	$\delta' c$	$U\delta' c$		δc	$U\delta c$	$\delta' c$	$U\delta' c$	
	/ (m s^{-1})				/ %			/ (m s^{-1})		/ %		
NaCl_5	1489.47	0.16	1.5	399	0.10	27	0.0	1.2	408	0.08	27	0.0
NaCl_10	1495.05	0.03	1.4	198	0.09	13	0.0	1.1	203	0.07	14	0.0
NaCl_15	1500.57	0.01	1.5	92	0.10	6.1	0.0	1.2	94	0.08	6.2	0.0
NaCl_20	1511.07	0.72	6.4	101	0.42	6.7	0.1	6.1	103	0.41	6.8	0.1
NaCl_25	1512.23	0.17	2.1	56	0.14	3.7	0.0	1.8	57	0.12	3.8	0.0
NaCl_30	1517.52	0.05	1.7	65	0.11	4.3	0.0	1.6	67	0.10	4.4	0.0
NaCl_35	1523.26	0.07	1.8	40	0.12	2.6	0.0	1.6	41	0.11	2.7	0.0
NaCl_40	1530.16	0.37	3.1	51	0.20	3.4	0.1	2.9	52	0.19	3.4	0.1

Table 4-13 DSA 5000 M Speed of sound results and respective uncertainty values

Samples codification	c_{DSA}	Uc_{DSA}	Deviation from Coppens Eq.				En	Deviation from UNESCO Eq.				En
			δc	$U\delta c$	$\delta' c$	$U\delta' c$		δc	$U\delta c$	$\delta' c$	$U\delta' c$	
	/ (m s^{-1})				/ %			/ (m s^{-1})		/ %		
OSIL_5	1489.35	0.13	1.3	367	0.09	25	0.0	1.0	376	0.07	25	0.0
OSIL_10	1494.54	0.01	0.7	183	0.05	12	0.0	0.4	188	0.03	13	0.0
OSIL_15	1500.05	0.18	0.6	90	0.04	6.0	0.0	0.3	92	0.02	6.2	0.0
OSIL_20	1507.41	0.80	2.4	99	0.16	6.5	0.0	2.1	101	0.14	6.7	0.0
OSIL_25	1510.34	0.01	-0.1	55	-0.01	3.6	0.0	-0.4	56	-0.03	3.7	0.0
OSIL_30	1515.84	0.10	-0.2	66	-0.02	4.4	0.0	-0.4	68	-0.03	4.5	0.0

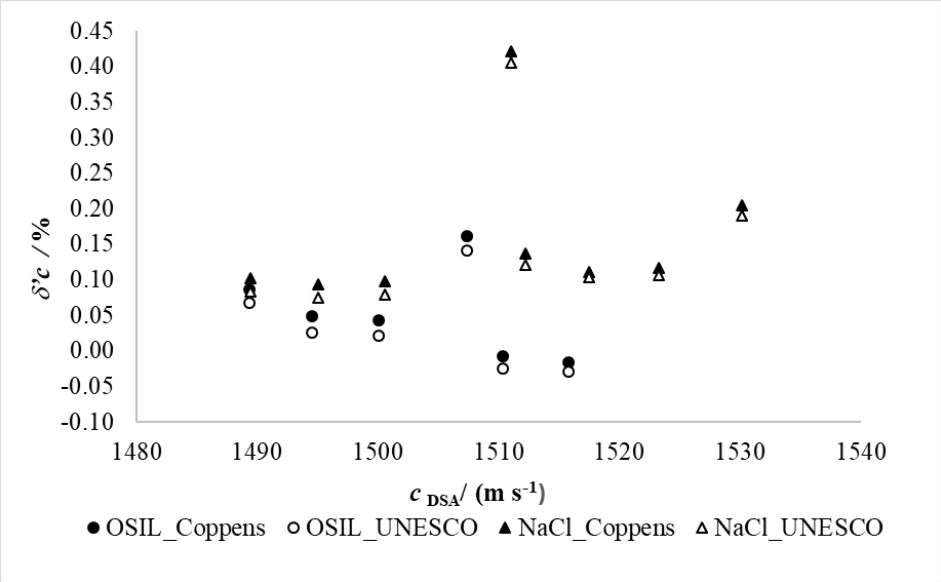

Figure 4-8 Speed of sound relative error versus speed of sound

4.2 Salinity determinations

The results of metrological compatibility of absolute salinity values, S_A obtained by refractometry and densimetry, investigated at 20 °C in the [5; 40] g kg^{-1} S_A interval, are given in Table 4-14. The obtained results were assessed by means of the normalized error, E_n, resulting from quotient of the difference of salinities ($|S_A(n) - S_A(\rho)|$) by expanded uncertainty of this difference ($\sqrt{U_{S_A(n)}{}^2 + U_{S_A(\rho)}{}^2}$. The results were satisfactory, i.e., $E_n \leq 1$, in the entire salinity range, meaning that these methodologies produce metrological compatible salinity results, both methodologies generate similar uncertainty values.

Table 4-14 Metrological compatibility of absolute salinity values and densimetry

Samples codification	$S_{A.\,nom.}$	$S_A(n)$	$U_{S_A(n)}$	$S_A(\rho)$	$U_{S_A(\rho)}$	δS_A	$U_{\delta SA}$	E_n
	/(g kg^{-1})							
NaCl_5	5	4.8	1.3	5.0	1.2	0.2	1.7	0.10
NaCl_10	10	10.2	1.2	10.1	1.2	-0.2	1.7	0.12
NaCl_15	15	15.12	0.86	15.00	0.82	-0.1	1.2	0.10
NaCl_20	20	19.9	1.2	20.0	1.2	0.1	1.7	0.03
NaCl_25	25	24.71	0.86	24.89	0.82	0.2	1.2	0.15
NaCl_30	30	29.5	1.2	29.9	1.2	0.4	1.6	0.25
NaCl_35	35	34.76	0.86	35.04	0.82	0.3	1.2	0.24
NaCl_40	40	39.8	1.2	40.0	1.2	0.2	1.7	0.09

The results of the study of the matrix effect on absolute salinity determination undergone with a set of standard seawater (SSW) samples of two different sources, both with a nominal S_A of 35 g kg^{-1}: OSIL and ERM, are given in Table 4-15. The salinity results obtained by both methodologies shown to metrological compatible as the ones obtained for sodium chloride solutions, rendering the matrix effect despicable.

Table 4-15 Metrological compatibility of results from refractometry and densimetry

Samples codification	$S_{A.\,nom.}$	$S_A(n)$	$U_{S_A(n)}$	$S_A(\rho)$	$U_{S_A(\rho)}$	δS_A	$U_{\delta SA}$	E_n
	/(g kg^{-1})							
SSW_OSIL_35	35	36.80	0.91	37.21	0.90	-0.4	1.3	0.32
SSW_ERM_35	35	36.09	0.88	35.68	0.83	0.4	1.2	0.34

5

CONCLUSIONS

This work allowed to validate IPQ's new density meter and speed of sound measurement system (Anton Paar, DSA 5000M) and to widen the salinity interval in which refractometry and densimetry could be used to determine salinity.

This density meter was able to measure density of sodium chloride solutions, at 20 °C, within the [1001, 1027] kg m^{-3} density interval, displaying density indication errors smaller than its uncertainty (0.020 kg m^{-3}). This means that there is no need to apply any correction to density indication values. It was also found that density indication errors without viscosity correction, δd_{nc}, were shown to be lower than the ones with viscosity correction, δd. In order to amend this situation, further investigations should be done together with the manufacturer, as the correction algorithm is not publicly available.

From the temperature calibration results, it was possible to establish a 0.038 °C tolerance for a [10, 40] °C interval.

Regarding the viscosity calibration, it was found that for viscosity corrected density indications, the errors can be considered neglectable for the [0.66, 70.32] mPa s viscosity interval, as the uncertainty is higher than the 0.050 kg m^{-3} deviation. For]70.32, 469] mPa s viscosity values, density errors reach a plateau with an around 0.106 kg m^{-3}maximum deviation. In future work, it is suggested to use lower uncertainties CRMs for the first interval.

The relationship between density indication errors and dynamic viscosity was investigated using polynomial regressions of the third order with DMA 5000M (Anton Paar) density meters (Furtado et al., 2017), effectively estimating the viscosity of Newtonian liquids within the [7, 220] mPa s viscosity interval, with a 3 % relative standard uncertainty. Employing this framework, correlations were established between dynamic viscosity and the error in the density indication values before viscosity correction (d_{nc}), as well as between D with error of the density indication values not viscosity corrected, d_{nc}. Utilizing this method, the dynamic vis-

cosity within the interval [0.65; 23.7] mPa s was estimated based on obtained D values. Calibration data facilitated the development of two third-degree polynomial curves of viscosity η versus D. The first curve encompassed the D interval [0; 0.000186] g cm^{-3}, corresponding to the dynamic viscosity interval [0.65; 23.7] mPa s, while the second curve covered the D interval]0.000186; 0.000550] g cm^{-3}, corresponding to the dynamic viscosity interval]23.7; 227] mPa s. The first curve enabled the estimation of dynamic viscosity from D with a relative expanded uncertainty of 12.7 %, while the second achieved 4.5 %. Comparing with prior studies (Furtado et al., 2017) where a 3 % relative standard uncertainty was attained for the viscosity interval of 7 mPa s to 220 mPa s, only the second interval demonstrated a relative uncertainty of a similar magnitude. This discrepancy may be attributed to the utilization of CRM with higher uncertainty in DSA 5000 M. Future endeavors might address this by adopting CRM with reduced uncertainties, especially those traceable to the hydrostatic weighing method for density determination, albeit a time-consuming technique.

The errors in speed of sound indication at 20 °C, within the [1255, 1484] m s^{-1} interval, can be considered negligible with a maximum deviation of 0.2 % when calibrated with degassed ultrapure water, n-Dodecane, and decane. These errors align within the range of uncertainty, which possesses a maximum deviation of 2.2 %. Going forward, this uncertainty value will serve as an acceptable tolerance level. Conversely, within the speed of sound interval of [1490, 1530] m s^{-1}, calibrated with aqueous solutions of NaCl and various dilutions of seawater prepared from OSIL SSW, relative errors derived from both reference equations (Coppens, UNESCO) range from 0.02 % to 0.42 %, with a relative expanded uncertainty of 2.6 % to 27 %. Notably, this higher uncertainty arises from the conversion of density to practical salinity associated with the reference values (refer to subchapter 2.2.4). Future work will aim to extensively explore the traceability of speed of sound measurement results across a wider range while endeavoring to reduce uncertainty through enhanced reference standards. Additionally, efforts will focus on establishing a reliable methodology for determining absolute salinity from speed of sound measurement results.

Finally, this work enabled to confirm the metrological compatibility of absolute salinity values, S_A, obtained by refractometry and densimetry in the [5; 40] g kg^{-1} S_A interval, including for seawater samples.

REFERENCES

Allen, J. T., Keen, P. W., Gardiner, J., Quartley, M. & Quartley, C. (2017). *A new salinity equation for sound speed instruments*. *Limnology and Oceanography*: *Methods*, 15(9), 810–820. https://doi.org/10.1002/lom3.10203

ANTON Paar GmbH (2023) *Basics of refractometry: Anton Paar Wiki*.. (2023). https://wiki.anton-paar.com/en/basics-of-refractometry/, accessed on 9/8/2023

ANTON Paar GmbH. (2021) *Instruction Manual and Safety Information DSA 5000M Density and Sound Velocity Meter instrument software version: from 2.98*, ANTON Paar GmbH.

Bettin, H., Borys, M. & Nicolaus, R. A. (2008). *Density: From the Measuring of a Silicon Sphere to Archimedes' Principle. Special Issue* / *PTB-Mitteilungen* 118, No. 2 and No. 3.

Bilaniuk, N. & Wong, G. S. K. (1993). *Speed of sound in pure water as a function of temperature. J. Acoust. Soc. Am.* 93(3) pp 1609-1612. as amended by N. Bilaniuk and G. S. K. Wong (1996). Erratum: Speed of sound in pure water as a function of temperature [J. Acoust. Soc. Am. 93. 1609-1612 (1993)]. J. Acoust. Soc. Am. 99(5). p 3257.

BIPM, IEC, IFCC, ILAC, ISO, IUPAC e OIML. 2008 *Evaluation of measurement data — guide to the expression of uncertainty in measurement,* JCGM 100: 2008 GUM 1995 with minor corrections. (Geneva: International Organization for Standardization) (Joint Committee for Guides in Metrology, JCGM 100:2008).

BIPM, JCGM 200:2012, *International Vocabulary of Metrology, Basic and General Concepts and Associated Terms*. VIM 3rd edition.

BIPM. (a) (2022) *SI promotion*. France

BIPM. (b) (2022) *SI brochure*. France

Bouchot, C., & Richon, D. (2001). *An enhanced method to calibrate oscillation tube densimeters. Fluid Phase Equilibria*, *191*(1–2), 189–208. https://doi.org/10.1016/s0378-3812(01)00627-6

California State University (2022). *17.3: Speed of Sound*. https://phys.libretexts.org/Bookshelves/University_Physics/Book%3A_University_Physics_(OpenStax)/Book%3A_University_Physics_I_-_Mechanics_Sound_Oscillations_and_Waves_(OpenStax)/17%3A_Sound/17.03%3A_Speed_of_Sound accessed on 16/6/2023

Chen, C.-T. & Millero, F. J. (1977). Speed of sound in seawater at high pressures. *The Journal of the Acoustical Society of America*, *62*(5), 1129–1135. https://doi.org/10.1121/1.381646

Coppens, A. B. (1981). *Simple equations for the speed of sound in Neptunian waters. The Journal of the Acoustical Society of America*, *69*(3), 862–863. https://doi.org/10.1121/1.385486

Ehlers, S., Könemann, J., Ott, O., Wolf, H., Šetina, J., Furtado, A., & Sabuga, W. (2019). *Selection and characterization of liquids for a low pressure interferometric liquid column manometer. Measurement*, 132, 191–198. https://doi.org/10.1016/j.measurement.2018.09.017

Feistel, R. & Gibbs, A. (2008). *Function for Seawater Dynamics for -6 ºC to 80 ºC and Salinity up to 120 g/kg.* Deep Sea Research I 55: 1639-1671.

Furtado, A., Napoleão, A., Pereira, J., Moura, S., Quendera, R., & Pellegrino, O. (2022). *Absolute salinity determination by oscillation-type densimetry and refractometry. International Journal of Metrology and Quality Engineering*, *13*, 10. ttps://doi.org/10.1051/ijmqe/2022007

Furtado, A. (2019). *Rastreabilidade Metrológica das Medições de Massa Volúmica e das Determinações Reológicas de Líquidos*, doctoral thesis FCT NOVA

Furtado, A., Pagel, R., Lorenz, F., Godinho, I., & Wolf, H. (2017). *Estimation of nominal viscosity of Newtonian liquids from data obtained by an oscillation-type density meter.* Ann. T. Nord. Rheol. Soc., 25, 321-8.

Furtado, A., Oliveira, C., Pellegrino, O., *et al*. (2013). *Metrological Compatibility of the Measurement Results of Aqueous Solutions Mass Fractions by densimetry and Refractometry*. IMEKO International TC8. TC23 and TC24 - 3rd Symposium on Traceability in Chemical. Food and Nutrition Measurements.

Furtado, A., Pellegrino, O., Alves, S., *et al*. (2010*). Determinação da fracção mássica de soluções aquosas de glucose por refractometria e densimetria de tubo vibrante*. In CONFMET2010

Gamsjäger, H., Lorimer, J. W., Scharlin, P., & Shaw, D. G. (2008). *Glossary of terms related to solubility* (IUPAC recommendations 2008). *Pure and Applied Chemistry*, *80*(2), 233–276. https://doi.org/10.1351/pac200880020233

Holcomb, C. D., & Outcalt, S. L. (1998). *A theoretically-based calibration and evaluation procedure for oscillation-tube densimeters*. *Fluid Phase Equilibria*, *150–151*, 815–827. https://doi.org/10.1016/s0378-3812(98)00362-8

IPQ (a)(2023). *Laboratorio Nacional*. https://www.ipq.pt/metrologia/laboratorio-nacional/ accessed on 3/8/2023

IPQ (b)(2023). *Propriedades de Líquidos*. https://www.ipq.pt/metrologia/medicoes-dominios-intervencao/areas-atividade/propriedades-de-liquidos/ accessed on 5/7/2023

IPQ (c)(2023). *Fotometria e Radiometria*. https://www.ipq.pt/metrologia/medicoes-dominios-intervencao/areas-atividade/fotometria-radiometria/ accessed on 25/5/2023

IPQ, (2012). *Vocabulário Internacional de Metrologia - VIM*, Instituto Português da Qualidade – IPQ

ISO 3696:1987 (1987) *Water for analytical laboratory use - Specification and test methods*

ISO 5725-2:1994*, Accuracy (trueness and precision) of measurement methods and results — Part 2: Basic method for the determination of repeatability and reproducibility of a standard measurement method*

ISO/IEC 17025:2017 *General requirements for the competence of testing and calibration laboratories*

Lagourette, B., Boned, C., Saint-Guirons, H. Xans, P. & Zhou, H. (1992). *Densimeter calibration method versus temperature and pressure. Measurement Science and Technology*, *3*(8), 699–703. https://doi.org/10.1088/0957-0233/3/8/002

Lemmon, E. W. & Huber, M. L. (2004). *Thermodynamic properties of n-dodecane. Energy & fuels*. 18(4). 960-967.

Lemmon, E. W. & Span, R. (2006). *Short fundamental equations of state for 20 industrial fluids. Journal of Chemical & Engineering Data*. 51(3). 785-850.

Marczak, W. (1997). *Water as a standard in the measurements of speed of sound in liquids. the Journal of the Acoustical Society of America*. 102(5). 2776-2779.

Millero, F. J., Feistel, R., Wright, D. G. & McDougall, T. J. (2008). *The composition of standard seawater and the definition of the reference-composition salinity scale*. *Deep Sea Research Part I: Oceanographic Research Papers*, *55*(1), 50–72. https://doi.org/10.1016/j.dsr.2007.10.001

Fofonoff, N.P. & Millard, Jr. R.C. *Algorithms for computation of fundamental properties of seawater (1983), UNESCO technical papers in marine science.* No. 44, Division of Marine Sciences. UNESCO, Place de Fontenoy, 75700 Paris.

Nayar, K. G., Sharqawy, M. H., Banchik, L. D. & Lienhard, V. J. H. (2016). *Thermophysical properties of seawater: A review and new correlations that include pressure dependence. Desalination*, *390*, 1–24. https://doi.org/10.1016/j.desal.2016.02.024

NOAA (2023). *All about the ocean*. Education. (National Geographic). https://education.nationalgeographic.org/resource/all-about-the-ocean/, accessed on 16/5/2023

NPL (2023). *Technical Guides - Speed of sound in sea water - Underlying Physics*. (2023). http://resource.npl.co.uk/acoustics/techguides/soundseawater/underlying-phys.html#up_coppens accessed on 1/9/2023

Pellegrino, O., Furtado, A. & Filipe, E. (2009). *Linear fitting procedures applied to refractometry of aqueous solutions. In: 3rd Symposium on Traceability in Chemical. Food and Nutrition Measurements*. Lisbon. Portugal. 6-11 September 2009. Proc. XIX IMEKO World Congress Fundamental and Applied Metrology.

Pellegrino, O., Furtado, A., Alves, S., Spohr, I. & Filipe, E. (2011a). *Compatibilidade metrológica de resultados de medição da fracção mássica de glucose em soluções aquosas por densimetria de tubo vibrante e refractometria. In 4.º Encontro Nacional da Sociedade Portuguesa de Metrologia*.

Pellegrino, O., Furtado, A., Alves, S., Spohr, I. & Filipe, E. (2011b). *Refractometria e densimetria de tubo vibrante: técnicas complementares na determinação da fracção mássica de glucose em soluções aquosas*. In XXII Encontro Nacional da Sociedade Portuguesa de Química.

Söhnel, O. & Novotný, P. (1985). *Densities of aqueous solutions of inorganic substances* (Vol. 22). Elsevier Publishing Company.

Stabinger, H. (1994). D*ensity Measurement using modern oscillating transducers*, South Yorkshire Trading Standards Unit, Sheffield.

Wolf, A. V. (1966). *Aqueous solutions and body fluids*. New York: Hoeber Medical Division.

Wong, G. S. & Zhu, S. (1995). *Speed of sound in seawater as a function of salinity, temperature, and pressure. The Journal of the Acoustical Society of America*, *97*(3), 1732–1736. https://doi.org/10.1121/1.413048